Relaxation to equilibrium of quantized chaotic states

A Thesis

submitted to
Indian Institute of Science Education and Research Pune
in partial fulfillment of the requirements for the
BS-MS Dual Degree Programme

by

Gowrisankar Aniruddhan

20121043

Certificate

This is to certify that this dissertation entitled Relaxation to equilibrium of quantized chaotic states towards the partial fulfilment of the BS-MS dual degree programme at the Indian Institute of Science Education and Research, Pune represents study/work carried out by G ANIRUDDHAN at Indian Institute of Science Education and Research under the supervision of ARUL LAKSHMINARAYAN, Professor, Department of Physics, during the academic year 2016-2017.

ARUL LAKSHMINARAYAN

G ANIRUDDHAN

Committee:
ARUL LAKSHMINARAYAN
M S SANTHANAM

To my parents and brother.

Declaration

I hereby declare that the matter embodied in the report entitled Relaxation to equilibrium of quantized chaotic states are the results of the work carried out by me at the Department of Physics, Name of the Institute, under the supervision of ARUL LAKSHMINARAYAN and the same has not been submitted elsewhere for any other degree.

ARUL LAKSHMINARAYAN

G ANIRUDDHAN

Contents

List of Figures

Abstract

Classical chaotic systems proceed to equilibrium by a mixing process in the phase space. We study this relaxation to equilibrium for quantized, bound chaotic maps on the torus. The *Ruelle-Pollicott* resonances that describe the mixing of classical chaotic system has been derived for the lazy-baker map, which is a non-uniformly hyperbolic system. The corresponding issue of quantifying mixing in Hilbert space has been discussed in this thesis and a correspondence between the classical and quantum relaxation has been shown for the same map. Later the effect of a random unitary transformation on the quantum relaxation has been shown to be an immediate relaxation to the equilibrium. An average of the quantum relaxation over all such random unitary transformations has been analytically performed. The average of the relaxation fluctuations about the equilibrium is derived to have a simple structure under certain conditions, reflecting the universal properties of the concerned random matrix ensemble.

Chapter 1

Introduction

Chaotic behavior in the physical world is ubiquitous, largely because of the underlaying nonlinearity. It has been known for a long time now that most natural deterministic systems around us also have this intriguing property, even in spite of them having very simple dynamics. In this sense, the term *chaos* is a misnomer. Intuitively, it sends across a image, which more often than not is associated with lack of information with regard to the system. However, that is not always the case, i.e determinism does not equate to predictability. "Deterministic chaos", as it is popularly termed is in some sense counter-intuitive. Even more surprisingly, chaos in natural systems seem to give rise to emergent properties that have unexpected regularity and universality. Studies have established correlations between spatiotemporal chaos and patten formation [2]. There has been much effort, cutting across disciplines to discern the underlying mechanism that give rise to such global patterns, so much so that Nonlinear studies have become commonplace in every area of research. However, mainstream appearance of chaos in Physics literature could be traced back more than a century ago to when Henri Poincaré in his quest to solve the famous three-body problem of the Sun-Earth-Moon system, glimpsed chaos at work. Since then, the study of chaos and it's intriguing properties has been a topic of research among mathematicians and physicists alike, the former providing a rigorous framework to effectively study various aspects of chaotic behavior. Over the years, notion of chaos in dynamical systems has been discussed by many authors, and much insight has been gained [3, 4]. With the advent of *Quantum mechanics* in the 20th century, a natural question was posed. Can Quantum mechanics reconcile with the phenomenon of chaos? or in other words, is there a Quantum analogue of classical deterministic chaos. Studies in this regard

have focused on Quantum systems that have a chaotic classical limit, to discern it's effects and have consequently lead to a new stream of research termed "Quantum chaos" or "Quantum chaology" [5]. For the purpose of this thesis, the former terminology has been used throughout. The reason for such a question, is the linearity of the Schrödinger equation which in essence does not entertain the phenomenon of *Sensitivity to initial conditions*, an important property of classical chaotic systems. Although many studies have probed the manifestation of chaos in Quantum mechanical systems, there is still not a clear mathematical or physical characterization of the phenomenon of chaos in quantum mechanics. Nevertheless, classical periodic orbits of chaotic systems have been used to give some analytical background in most situations and come broadly under the purview of *Periodic-orbit theory*. Such studies have been broadly classified as *Semiclassical*. There have also been studies which establish equivalence of the energy spectrum of the quantized systems and Random Matrix theory ensembles [6,7], thus providing a statistical framework to deal with the energy levels. In particular based on the properties and symmetries of the quantum systems, they reflect the properties of one of three random matrix ensembles, namely the *Gaussian orthogonal ensemble*(GOE), the *Gaussian unitary ensemble*(GUE) or the *Gaussian symplectic ensemble*(GSE). *Entangling power* of quantum chaos [8] and study of decoherence in quantum systems [9,10] are two hot research topics in quantum chaos, especially because of their importance to realizing a quantum computer. One of the major hurdles in the study of Quantum chaos is the fact that "*quantization*" of classically chaotic systems is often not straightforward.

Simple exactly solvable Hamiltonian systems exhibiting classical chaos have been very instrumental in the study of chaos, both in understanding it's classical complexity and in determining it's quantum manifestation. Arnold's cat map, baker map, kicked Hamiltonian systems and dynamical billiards are some examples of quintessential models used in the study of Quantum chaos. In particular, the baker map is an abstract map with no generating Hamiltonian. It is special because of the underlying simplicity in dynamics that exemplifies the genesis of chaos in the phase space, namely the *homoclinic tangle*, first illustrated by Poincaré himself. In the subsequent sections, various aspects of the baker map have been discussed including it's quantization [11,12]. Kicked Hamiltonian systems also hold a special place in the study of Quantum chaos. These are Hamiltonian systems with a potential that is periodically switched on and off, termed as a "*kick*". In particular, the special class of "1.5 de-

grees of freedom" (non-autonomous 1 DOF) systems have been extensively studied, popular examples being the *kicked pendulum* a.k.a *Chirikov-standard map* [13,14] and the *kicked Harper map* [15]. Their dynamics can be faithfully described by an area preserving map in the position and momentum coordinates termed as a *stroboscopic mapping*. More importantly, the quantization of such kicked systems is straightforward as described in the subsequent chapter [16]. In this thesis we have used three models, two of them being based on the *baker map*, namely the *three-baker* [17] and the *lazy-baker* [18]. The third model we have used in this thesis is the *standard map*.

Study of deterministic chaos in dynamical systems has led to a hierarchical structure, as prescribed by the *ergodic hypothesis*, with Ergodic systems at the lower end of the chaotic spectrum. One classic interpretation of the hierarchy is through the notion of unpredictability which can be viewed as a decay of correlation between two subsets of phase space [19]. In the case of Hamiltonian systems, this can be visualized as a mixing on the energy shell in phase space, with the area as the invariant measure (μ). However, quantum dynamical systems do not have such a definite hierarchy and the corresponding issue of quantum mixing is difficult to analyze. In this thesis we quantify the *mixing* in Hilbert space by using projectors and study various properties of it. The study has focused only on simple Hamiltonian systems that show *hard chaos*. In particular, two-dimensional area preserving maps that are quantized on the unit torus have been used. The Hilbert space is consequently finite dimensional, with the scaled Plank's constant defined as the inverse of the dimensionality, $h = \frac{1}{N}$. Classically, we have quantified the mixing in phase space by the correlation between two initially disjoint and uniform phase space densities as a function of time. One of the densities is evolved in time and the overlap of this with the other is studied. In the study of dynamics systems, this mixing has been quantified by the *Ruelle-Pollicott* (R-P) resonances [20]. Correspondingly, in the quantum case the overlap of two *orthogonal* projectors in the Hilbert space with one of them iterated in time is studied as the analogue of the correlation. One of the motivations of this study was to probe if there are any quantum signatures of the classical RP-resonances. To this effect, the action of a random unitary operation on the relaxation have been studied, which are shown to erase any resemblance of such a signature that was observed. The quantum correlation in this case averaged over the *haar* measure of the unitary group has also been calculated analytically, with interesting universal properties specific to the random matrix ensemble of the quantum system. ruellIt remains to be seen, if

a connection can be made to the literature on scrambling of quantum information, which is quantified by an out-of-time-order correlation, that is seen to have a similar structure to the quantum correlation function. [21].

1.1 Classical Hamiltonian chaos

The term *chaos* has come to be somewhat of a commonality in the scientific community, primarily due to the much celebrated *butterfly effect*. Aided by the fast paced growth of computing facilities and performance, the ubiquity of chaos has been appreciated across all disciplines. Mathematicians have provided a very rigorous framework to treat dynamical systems. Such a mathematical definition of chaos by Devaney [22] states that a dynamical system (X, f), $f : X \to X$ is chaotic provided,

1. f **is sensitive to initial conditions**: if there exists $\delta \geq 0$ such that, $\forall\ x \in X$ and any neighborhood N of x, $\exists\ y \in N$ and $n \geq 0$ such that $|f^n(x) - f^n(y)| \geq \delta$

2. **Topological transitivity**: if for any pair of open sets $U, V \subset X$, there exists $k \geq 0$ such that $f^k(U) \cap V \neq \emptyset$.

3. **Dense periodic orbits**: if arbitrarily close to any point on a periodic orbit in phase space, there exists another periodic orbit.

Aptly summarized by Devaney, chaotic behavior has three components:"*unpredictability, in-decomposability and an element of regularity*". In the above definition, f can be a continuous flow or an iterated mapping. However, for the purpose of this thesis we are only interested in the latter. One important parameter characterizing sensitivity to initial condition is the *Lyapunov exponent*, which is a measure of the mean exponential divergence of trajectories. Having defined chaos we will take a short detour over the key aspects of classical Hamiltonian chaos that would prove essential.

Given a dynamical system described by a Hamiltonian with d DOF, the phase space of the system is 2d dimensional in position and momentum variables, (q_i, p_i). The equations of motion are prescribed by Hamilton's equations.

$$\dot{q}_i = \frac{\partial H}{\partial p_i}\ ;\ \dot{p}_i = -\frac{\partial H}{\partial q_i} \tag{1.1}$$

These differential equations can be regarded as a vector field that describe an incompressible flow in the $2d$ dimensional phase space, thanks to the Liouville equation. A

dynamical systems is defined to be a Hamiltonian system, if the Hamiltonian H is constant in time. In such a case, the Hamiltonian is said to be a constant of motion. This constant of motion defines a surface on the $2d$ dimensional phase space, on which the system is restricted to reside. Apart from the Hamiltonian, a system can have other constants of motion. If T_i is said to be a constant of motion, then it is easy to see that $\{T_i, H\} = 0$. A dynamical system with d DOF is said to be integrable, if there are d constants of motion. If this is the case, then the system permits good action-angle variable, where the Hamiltonian is a function of only the action and the dynamics of the system is said to be confined to a d-dimensional invariant tori. The action-angle variables are just canonical transformation of the original phase space variables. However, it is often not straightforward to find the transformation or the constants of motion, given a dynamical system. If the dynamics of the system does not allow d constants of motion, it is said to be non-integrable and the system invariably shows chaotic behavior.

It is straightforward to see that 1 DOF systems are always integrable. The Hamiltonian is the only constant of motion and hence trivially integrable. For systems with more than 1 DOF, it is known that they are neither completely integrable nor are they completely chaotic [23]. For the sake of simplicity, let us take the example of a system with 2 DOF. This means that the phase space is 4 dimensional. Hamiltonian systems are restricted to the energy shell in phase space, in this case which is 3 dimensional manifold. The visualization of the dynamics of the system is even more simplified by Poincaré's prescription of studying the *surface-of-section*. Instead of studying the flow in the energy shell, the intersection of the flow with a surface of lower dimension is studied, in this case a plane. This way, the dynamics of a 2 DOF Hamiltonian system is studied on a 2 dimensional phase space, with mappings from one intersection to the next. This is extended to the case of 1 DOF periodically forced Hamiltonian systems, where the mapping corresponds to two points spaced one time period of forcing apart. These are popularly called *stroboscopic maps* and the systems are collectively referred to as 1.5 DOF systems, being the simplest of systems exhibiting chaos. Such maps belong to the category of 2-dimensional area preserving maps.

The 2-dimensional area-preserving map can be defined as, $(q_{k+1}, p_{k+1}) = M(q_k, p_k)$, where (q_k, p_k) is the k'th iterate starting from a given initial point. In fact, given an initial point, a bi-infinite sequence of iterates can be found extending both forward

and backward in time, the latter of which will be useful in defining some important features. If we denote the k'th iterate by T_k, the bi-infinite sequence can be represented as $(...T_{-2}, T_{-1}, T_0, T_1, T_2...)$. In systems which permit *symbolic dynamics*, each point by itself encodes the trajectory or in other words, the bi-infinite sequence. Important features of such maps are periodic orbits, stable/unstable manifolds and homoclinic/heteroclinic orbits

1. **Periodic orbits**: An orbit is termed to be periodic with period n if $T_{k+n} = T_k$ for all values of k. When $n = 1$, it is called a fixed point of the map.

2. **Unstable/Stable manifold**: Set of points that approach a hyperbolic periodic point, x^* in the distant past/far future and denoted by $W^u(x^*)/W^s(x^*)$. These are collections of orbits that do not self-intersect.

3. **Homoclinic/Heteroclinic orbits**: Orbits that approach the same/different periodic orbits in the distant past and future. These orbits are formed by the intersection of a stable and an unstable manifold.

Although the stable and unstable manifolds cannot self-intersect, they can intersect one-another giving rise to homoclinic and heteroclinic orbits. Given that they intersect once, all of it's iterates are also have to be intersections due to continuity of the transformation. This along with the area-preserving nature of the transformation results in a very complicated structures, termed the *homoclinic tangle*. Phase space points in such a region seem to behave randomly, although their dynamics is completely deterministic. The *homoclinic tangle* in some sense, can be perceived as the genesis of Hamiltonian chaos. Poincaré himself was probably the first to appreciate the underlying complexity in his treatise, "Les méthodes nouvelles de la méchanique céleste" in 1899. Having discussed Hamiltonian chaos in brevity, we will subsequently describe the models we have used in this study.

1.2 The baker map

As explained in the previous section, the baker map is an abstract map with no generating Hamiltonian. The dynamics of the map is similar to the Smale-horseshoe map [22]. It is celebrated as one of most simplest dynamical system that is exactly solvable and exhibiting *hard chaos*. The baker map is defined on the unit square

as [24],

$$B(q,p) = \begin{cases} (2q, p/2) & 0 \leq q < \frac{1}{2} \\ (2q-1, \frac{1}{2}(p+1)) & \frac{1}{2} \leq q < 1 \end{cases} \tag{1.2}$$

Although the exactly solvable part will become apparent subsequently, it is helpful

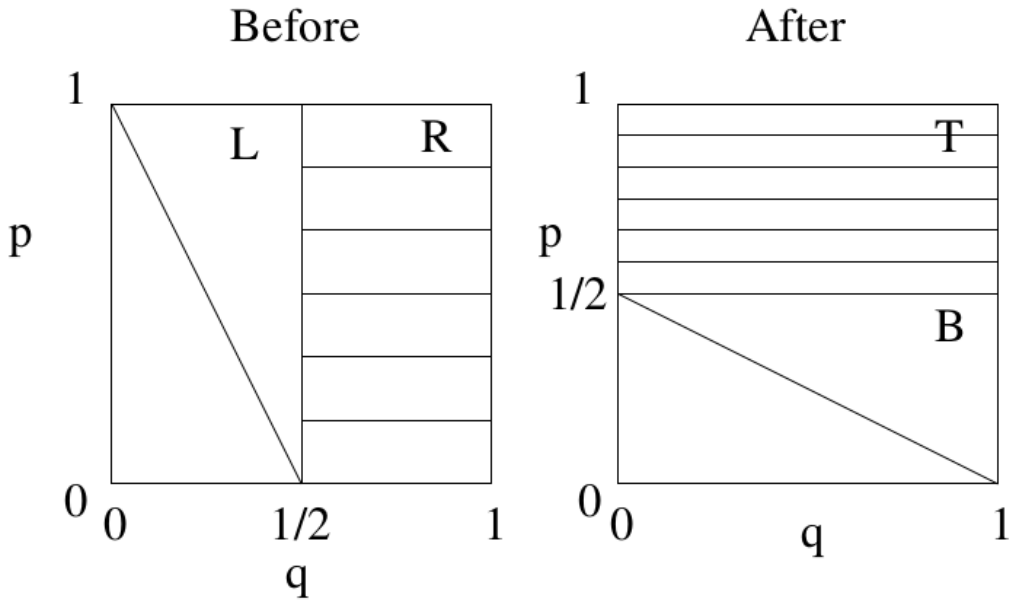

Figure 1.1: A figure illustrating the action of the baker map on the unit square [1]. The figure clearly shows the stretching along the position axis and compression along the momentum axis.

to note that dynamics depends only on the position coordinate, q. In short, we solve for q, we can solve the baker map. The dynamics of the position, q alone is identical to that of the *shift map* defined as $S(q) = 2q(mod1)$ and is exactly solvable. The action of the baker map can be visualized as a stretching in the q-axis and a compression along the p-axis by factors of 2 and 1/2 respectively. It's action is very similar to a kneading action of a baker on the batter, hence the name. Evaluating the Jacobian, it is straightforward to find the eigenvalues to be 2 and $\frac{1}{2}$, hence it is uniformly hyperbolic. The Lyapunov exponents calculated as the logarithm of the eigenvalues, are $\pm\log(2)$. The largest Lyapunov exponent describes the dynamics of the systems and the one positive Lyapunov exponent in this case is indicative of chaos. However, the description in it's present form does not offer any insight into it's chaotic behavior. Fortunately, the system allows the definition of a *Symbolic*

dynamics. Symbolic representation of the dynamics is considered a powerful tool in the study of dynamical systems, where each point of the phase space is encoded by a sequence of symbols with the dynamics represented by a shift map. It is important to note that not all systems allow an easy definition of the dynamics symbolically. In the case of the baker map, this involves expressing the position and momentum in binary, $p = 0.b_1b_2b_3b_4b_5....$ and $q = 0.a_1a_2a_3a_4....$, where $a_i, b_i \in \{0, 1\}$ Using this construct, any point on the phase space is represented by a bi-infinite sequence of binary digits as $(p|q)$ where,

$$(p|q) = ...b_3b_2b_1 \cdot a_1a_2a_3.... \tag{1.3}$$

In the binary representation, it is apparent that $q \geq \frac{1}{2}$, if $a_1 = 1$ and 0 otherwise. The simplicity of the dynamics becomes apparent if the action is represented one-by-one.

$$2q(mod1) = a_1.a_2a_3a_4....(mod1) = 0.a_2a_3a_4.... \tag{1.4}$$

$$\frac{1}{2}p = 0.0b_1b_2b_3b_4.... \tag{1.5}$$

Since $a_1 = 0$ or 1 defines whether the point lies to the left half or right half of the position axis, the action of a single iteration can be represented "symbolically" as a *left-shift* of the bi-infinite sequence representing a point.

$$B(p|q) = B(....b_4b_3b_2b_1 \cdot a_1a_2a_3a_4....) = ...b_4b_3b_2b_1a_1 \cdot a_2a_3a_4.... \tag{1.6}$$

The dynamics is isomorphic to a Bernoulli shift [24] and therefore shows *hard chaos*. Now it becomes easy to see that the baker map is exactly solvable. In short, the entire orbit is specified once a point is specified and is encoded in it's binary representation. It also becomes easy to analytically define periodic orbits. Let us first define u_k to be a sequence of k binary digits, i.e $u_k = x_1x_2x_3.....x_k$. We define a periodic point as $B^k(p_0|q_0) = (p_0|q_0)$. Therefore, $(p_0|q_0) = ...u_ku_k \cdot u_ku_k...$ defines a periodic orbit of period k. Similarly, it is straightforward to describe stable/unstable manifolds and consequently homoclinic/heteroclinic orbits.

The classical baker map defined above has two fundamental symmetries, *reflection* and *time-reversal* symmetry. Reflection is defined as $R(q, p) = (1 - q, 1 - p)$, i.e the reflection of a point about the center. In symbolic dynamics, R is just the conjugation operation, and this does not affect the left-shift of the baker map. Therefore R and B

commute, i.e $R \circ B = B \circ R$, and hence it is symmetry of the baker map. Time-reversal, T on the other hand is defined by the interchange of the position and momentum, i.e $p \leftrightarrow p$ and $t \rightarrow -t$. T represents an inversion of the bi-infinite sequence, and the inverse mapping will indeed be equivalent to the forward mapping without T, i.e $T \circ B = B^{-1} \circ T$. Therefore, the baker map also has time-reversal symmetry, T. In the next chapter, we will look at models that are slight modification of this map and their corresponding quantization.

1.3 The standard map

$$H = f(p) + V(q) \sum_{n=-\infty}^{\infty} \delta(t/T - n) \tag{1.7}$$

The above equation illustrates the general form of *kicked* Hamiltonian systems. The summation over the delta functions acts as the *kick* with time period T and can be collectively represented as $\delta_T(t)$. $f(p)$ acts as the kinetic term and $V(q)$, the potential. The corresponding equation of motion is given by

$$\dot{q} = \frac{\partial H}{\partial p} = \frac{df(p)}{dp} = f'(p) \tag{1.8}$$

$$\dot{p} = -\frac{\partial H}{\partial q} = -\delta_T(t)\frac{dV(q)}{dq} = -\delta_T(t)V'(q) \tag{1.9}$$

As discussed in the previous sections, the dynamics of this Hamiltonian can be represented by a two-dimensional map of q and p between successive kicks called the **Stroboscopic map**. Consider the initial point (q_i, p_i) to be immediately after the i'th kick. Clearly, between the delta kicks, the Hamiltonian just has the kinetic term and time derivative of p is 0. Hence the momentum remains a constant between the kicks. Therefore, the position immediately before the next kick, q_{i+1}^- can be found by a simple direct integration. Integrating the position across the infinitesimal width of the delta function will in essence have no contribution, i.e $q_{i+1} = q_{i+1}^-$, provided f is a smooth function itself. However, the integration of the momentum across the delta kick does indeed have a contribution because of it's mathematical structure.

$$q_{i+1} = q_i + Tf'(p_i) \tag{1.10}$$

$$p_{i+1} = p_i - TV'(q_{i+1}) \tag{1.11}$$

A popular example is the *standard map*, where $f(p) = \frac{1}{2}p^2$ and $V(q) = -\frac{k}{4\pi^2}\cos(2\pi q)$. Where $q \in [0, 1]$ is an angle like variable and the constant term k is the strength of the potential kick. The stroboscopic map for the case when $T = 1$ is given by,

$$q_{i+1} = q_i + p_i (mod 1) \tag{1.12}$$

$$p_{i+1} = p_i - \frac{k}{2\pi}\sin(2\pi q_{i+1}) \tag{1.13}$$

The modulo 1 operation ensures that the position coordinate is cyclic and the phase space is restricted to be a cylinder. It is also easy to see that translation of momentum by unity is a symmetry of the map. Therefore, a modulo 1 operation on momentum can also be imposed to observe it's dynamics restricted to a torus phase space. By varying the parameter k, we can effectively transition from a perfectly integral case($k = 0$) to completely chaotic case($k > 7$) (fig.1.3). The transition to chaos is as prescribed by the Kolmogorov-Arnold-Moser (KAM) and Poincaré-Birkhoff (PB) theorem, by effectively treating the potential as a perturbation. The parameter k thus acts as the strength of the perturbation. When $k = 0$, the map is perfectly integrable and identical to the popular "twist-map". As the value of k increases, the rational tori give rise to chain of alternating periodic and hyperbolic points as prescribed by the PB theorem. The fate of the irrational tori on the other hand is as prescribed by the KAM theorem and survive for sufficiently small perturbation. The parameter k is such that the last KAM invariant tori breaks at the "golden mean", i.e $k \approx 0.97..$ [25]. The breaking of the last KAM tori allows signifies the beginning of global diffusion over the phase space and hence global chaos. This is clearly evident in fig. 1.3 where phase space becomes more and more random with increasing k. In the case when the momentum is unbounded and the phase space becomes a cylinder, the dynamics of the map shows a diffusion in the momentum direction, identical to a random walker on the real line. The standard map was one of the earliest models to be quantized. On quantizing this map, it was found that the classical diffusion was suppressed, which led to the usage "quantum suppression of classical chaos".

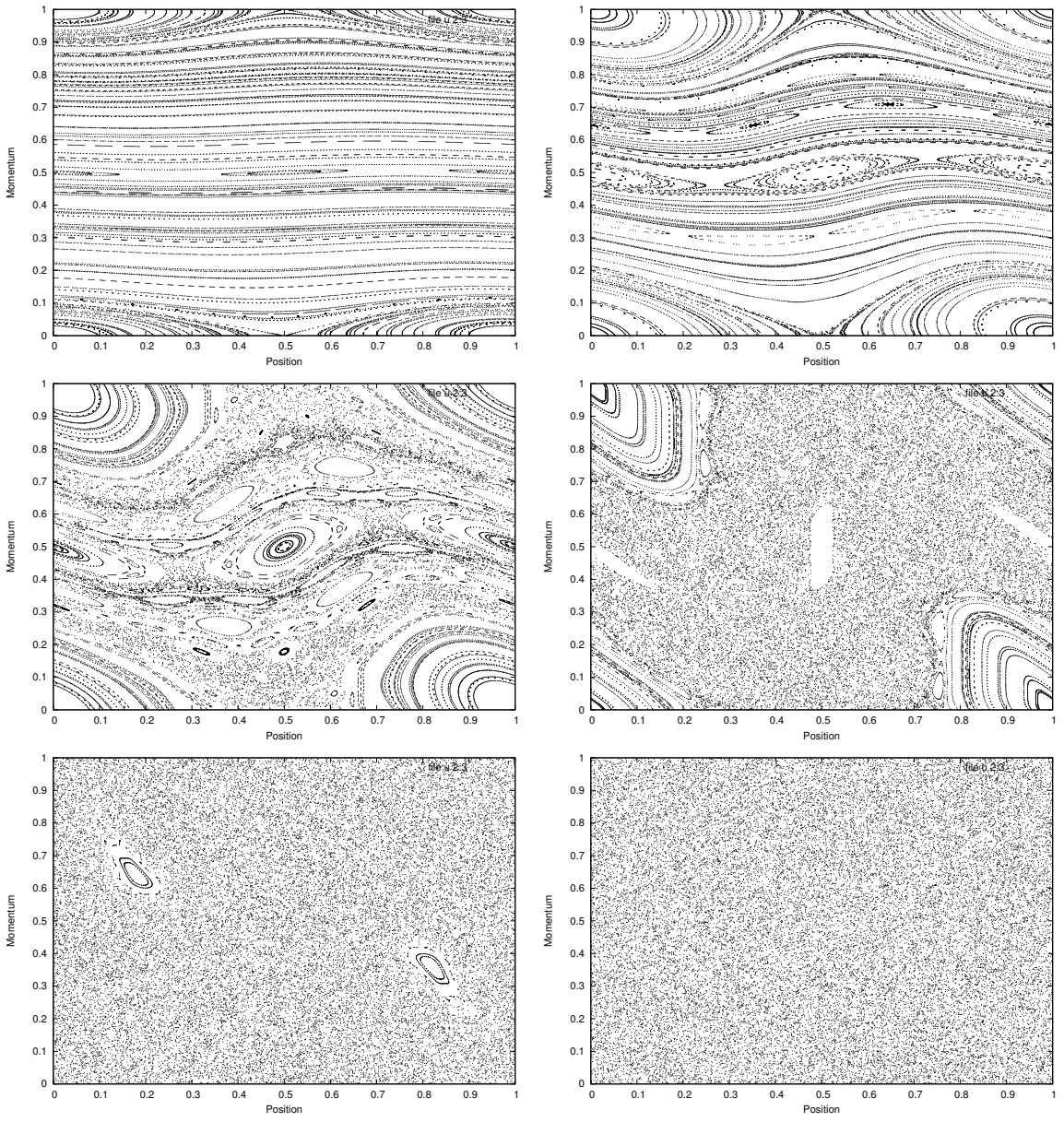

Figure 1.2: Phase space plots of the standard map for values of k=0.1,0.5,1,2,5 and 7 in ascending order from top left to bottom right. The plots are generated by taking 100 random initial values iterated for 300 time steps.

Chapter 2

Methods

2.1 Classical relaxation

Quantification of the classical relaxation of dynamical systems has been done by characterizing the mixing in phase space. This has been studied before and we use a formulation similar to that used in ref. [26] to study the relaxation towards equilibrium. Consider a set Ω, which we shall call the phase space. A σ-algebra of Ω is the collection of subsets of Ω including the null set, that is closed under (a)complement, (b)countable unions and (c)countable intersections of it's elements. Let us denote this as Σ. The set Ω and it's σ-algebra Σ are set to constitute a *measurable* space. Let us now define the dynamical system to be $[\Omega, \Sigma, \mu]$, where Ω is the phase space, Σ is the σ-algebra of Ω and μ is the measure on Ω. μ is said to be a probability measure if $\mu(\Omega) = 1$. Let the dynamics of the systems be described by a flow, $f : \Omega \to \Omega$ such that $\forall\ c \in \Sigma$, we have $\mu(f^{-1}c) = \mu(c)$(measure preserving) [19] . Given this definition, a dynamical system is said to be completely mixing if,

$$\lim_{n\to\infty} \mu\left(f^n A \cap B\right) = \mu(A)\mu(B)\ ,\ \forall\ A, B \in \Sigma \tag{2.1}$$

We use this as our starting point to quantify the relaxation between two subsets of the phase space, denoted by A and B. The mixing of A and B can be calculated using either characteristic phase space function or uniform phase space densities localized to A and B, both of which are interrelated. We will proceed by using the former, as it is more intuitive. A characteristic function of a subspace is a piecewise function whose value is 1 inside the corresponding subspace and 0 everywhere else. The integral of a

characteristic function over the phase space is the measure of the subset it represents. Let χ_A and χ_B denote the characteristic functions over A and B respectively. From the definition of $\chi_{A/B}$, it is clear that

$$\int\int \chi_B \cdot (f^t \cdot \chi_A)\ dqdp = \mu(f^t A \cup B) \tag{2.2}$$

To quantify the amount of mixing with time, we define the correlation function, $c(t)$ as the measure of the overlap of subset A iterated in time with the subset B, suitably normalized for the choice of A and B.

$$c(t) = \frac{\mu\left(f^t A \cup B\right)}{\mu(A)\mu(B)} \tag{2.3}$$

$$\implies \lim_{t\to\infty} c(t) = 1 \tag{2.4}$$

where, eqn. 2.1 has been used to derive the final expression. In the theory of dynamical systems, the decay of the above correlation for any *mixing* system is dictated by a set of complex numbers called the "*Ruelle-Pollicott*(R-P) resonances" [20, 27]. The R-P resonances for any given system are not easy to calculate.

$$\frac{\mu\left(f^t A \cup B\right)}{\mu(A)\mu(B)} - 1 = \sum_i p_i \exp(\lambda_i) \tag{2.5}$$

where $p_i's$ are just the coefficients. In the case of the triple-baker and lazy-baker, these resonances, λ_i could be explicitly calculated using the fact that they were "*isomorphic to a finite time Markov process*" [26] and constructing subsets A and B such that they were easily representable as probability vectors using Markov partitions. The representation in terms of the Markov partitions is analogous to the usage of characteristic functions, and hence the equivalence in describing the relaxation.

Let us assume that Markov partitions for a given map has been defined. Let the partitions be numbered and be denoted as Q_i, which is the $i'th$ partition. We will now define a Markov matrix as a matrix whose elements are basically the transition probability amplitudes from one partition to another. Let us say we start with a uniform probability distribution over partition Q_k, with an associated measure/probability $p_k = \mu(Q_k)$. Let the partition Q_k be iterated for one time step and let the overlap of the iterated partition Q_k with another partition Q_l be Q_{lk}. The transition amplitude from Q_k to Q_l is given by $m_{lk} = \mu(Q_{lk})/\mu(Q_k)$. Thus the partitions iterated once

in time, will give us the Markov matrix, In the case of 2D area preserving maps the measure is simply the area of the phase space. Therefore, we can derive the Markov matrix, M from simply the overlapping area of two partitions over a single time step. Subsequently, we will define two classical maps and their corresponding Markov partitions. We will use this matrix M to derive the relaxation law for the corresponding map.

2.2 Classical three-baker map

The three-baker a.k.a interacting baker map is a simple variant of the classical baker map. The interacting/three-baker was first studied by Elskens and Kapral as a model for studying chemical rate laws [28] and have been shown to be completely mixing. This model was later quantized by Lakshminarayan to study it's relaxation to equilibrium [17]. The classical relaxation law had been derived analytically in the same article, using *Markov* partitions. Markov partitions are tools to describe the dynamics of a system as discrete time Markov shift process, popularly termed as *Symbolic dynamics*, which was mentioned in conjunction with the baker map earlier. Subsequently, we will briefly describe the process.

The phase space of the three-baker is taken to be the unit square divided into two equal halves along the position. Two independent "bakers", A and B, defined suitably are placed on the two halves and a third one, C is placed overlapping the two equal halves, with the parameter α defining the extent of the overlap (fig 2.2). The action of the map is such that there is perfect mixing by bakers A and B in their respective cells without any mixing between them. The baker in C perfectly mixes a portion of A and B, thus facilitating the interaction. Therefore, the classical map, can be expressed as $M_\alpha = B_C B_{AB}$. The bakers on A and B commute since they are disjoint and hence represented together as B_{AB}. The function B_C depends on the parameter α which defines the boundary of the C portion.

$$B_C^\alpha(q,p) = \begin{cases} (2q - (1-\alpha)/2, p/2), & (1-\alpha)/2 \leq q < 1/2 \\ (2q - (1+\alpha)/2, p/2), & 1/2 \leq q < (1+\alpha)/2 \end{cases}$$

For a given rational value of $\alpha = \frac{a}{b}$, $2b$ equal vertical strips along the position axis constitute the Markov partitions. In the previous section, we have defined the

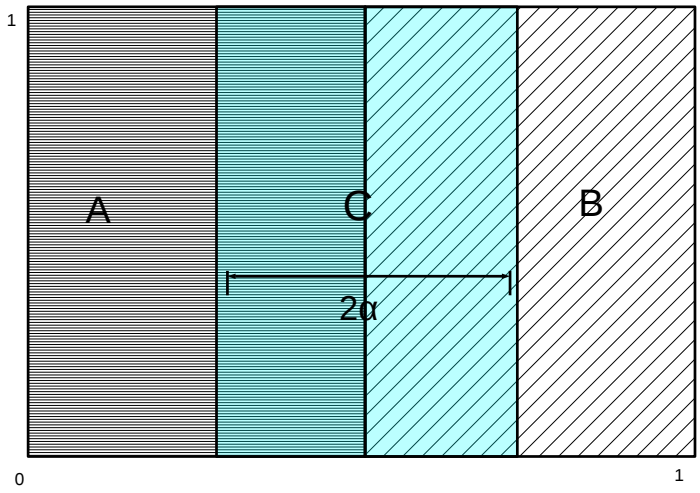

Figure 2.1: Phase space of the three-baker illustrating the three partitions along with the parameter α.

Markov matrix and using the same definition, we can find the Markov matrix for a given value of α. For example, let $\alpha = \frac{1}{2}$. This implies that the phase space is divided into 4 equal vertical strips (fig.2.2). The corresponding Markov matrix is given by,

$$M = \begin{pmatrix} 1/2 & 1/2 & 0 & 0 \\ 1/4 & 1/4 & 1/4 & 1/4 \\ 1/4 & 1/4 & 1/4 & 1/4 \\ 0 & 0 & 1/2 & 1/2 \end{pmatrix}$$

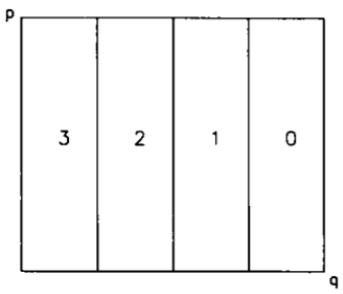

Figure 2.2: Markov partitions for the three-baker

The eigenvalues of the matrix M are 1 and $\frac{1}{2}$. Let A and B be the left and right halves of the phase space. We shall denote A as a probability vector in terms of the Markov partitions, i.e $P_A = (0, 0, \frac{1}{2}, \frac{1}{2})^\intercal$. Now P_A iterated in time is $M^t \cdot P_A = (f_1, f_2, f_3, f_4)^\intercal$. The $f_i's$ denote the fraction of A in the $i'th$ partition after t iterations. Let us now represent B as a projector in terms of the Markov partitions, i.e $P_B = (1, 1, 0, 0)$. Thus $P_B \cdot M^t \cdot P_A$ is the sum of fractions of A in B. This multiplied by the measure of A is the measure of the overlap, $\mu(A^t \cap B)$.

Therefore, the classical correlation, $c(t)$ is given by,

$$c(t) = \frac{1}{\mu(B)} P_B \cdot M^t \cdot P_A = 1 - (1/2)^t \tag{2.6}$$

2.3 Classical lazy-baker map

The lazy-bakers are a class of maps on the torus that are area-preserving, not completely hyperbolic with dynamics that includes geometric actions of rotations apart from the stretching and folding of the baker map. This gives rise to models, whose dynamics range from completely regular to fully ergodic. This class of systems, termed SRS maps were first introduced and quantized by Lakshminarayan and Balazs [18]. However, in this thesis we are only interested in a special case of SRS, termed the SR map. The map is defined on the unit-square and is area-preserving. The unit square is divided into two halves with the usual stretching on the left side and a rotation by $\pi/2$ of the right side.

$$B_{lb}(q,p) \rightarrow \begin{cases} (q/2, 2p) & \text{if } 0 \leq q \leq 1/2 \\ (1-p, q) & \text{if } 1/2 < q \leq 1 \end{cases}$$

The dynamics of the lazy-baker can also be represented symbolically, by representing

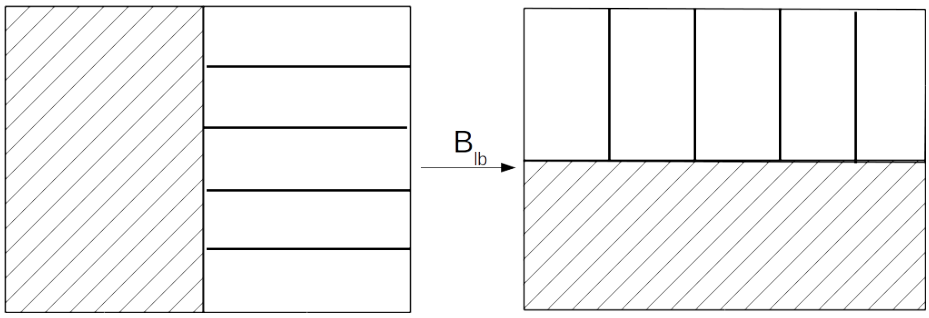

Figure 2.3: Figure illustrating the disparate action of the lazy-baker on the left and right halves of the unit-square. There is a stretching on the left and rotation on the right half.

the position and momentum in binary and using a similar representation of the phase space point as that of the baker map,$(p|q)$(1.3). It was shown in [18], that the symbolic dynamics of the lazy-baker was one of eventual left-shift, similar to the classical baker map. Therefore, the SR map is a chaotic map on the whole measure. Also the largest

Lyapunov exponent of the lazy-baker was shown to be $\frac{1}{2}log(2)$, exactly half of the normal baker map. Thus the rate of exponential divergence of nearby trajectories is also slower than the baker map, hence the name. The "*laziness*" of this map gives us the opportunity to observe it's mixing in phase space. The Markov partition for the lazy-baker can be constructed and it's relaxation laws can be found using the same. The Markov partitions for the lazy-baker are presented in the figure to the right and it's corresponding Markov matrix is,

$$M = \begin{pmatrix} 1/2 & 1 & 0 \\ 0 & 0 & 1 \\ 1/2 & 0 & 0 \end{pmatrix}$$

The eigenvalues of this matrix are 1, λ and λ^*, where $\lambda = \frac{1+i\sqrt{7}}{2}$.

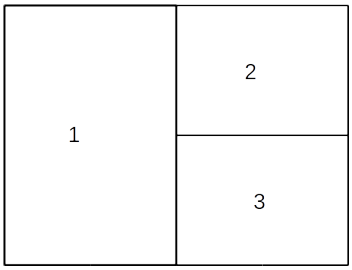

Figure 2.4: Markov partitions for the lazy-baker

Using the same example, let A and B denote the left and right halves of the phase space respectively. Let us denote A as a probability vector in terms of the Markov partitions, $P_A = (1, 0, 0)^\intercal$. Once again let $P_t = M^t \cdot P_A$, where $P_t = (f_1, f_2, f_3)^\intercal$, with f_i's denoting the fraction of A present in the respective partitions after t iterations and $\sum f_i = 1$. Representing B as a projector in terms of the Markov partitions, $P_B = (0, 1, 1)$, we can now calculate the fraction of A in B by calculating $P_B \cdot M^t \cdot P_A$. Similarly, this quantity times $\mu(A)$ gives the measure of the overlap, $\mu(A^t \cap B)$. Therefore we can calculate the classical relaxation law using the above expression to be,

$$c(t) = \frac{1}{\mu(B)} P_B \cdot M^t \cdot P_A = \left(1 - a\lambda^t - a^*(\lambda^*)^t\right) \tag{2.7}$$

where $a = (1/2 - 0.18898i)$ and λ, λ^* are the eigenvalues of the matrix M, mentioned above. On comparing this with eqn.2.5, we can see that the Ruelle-Pollicott resonances for this map are just the natural logarithm of λ and λ^*. The values of a are dependent on the particular choice of A and B.

2.4 Quantum maps

Quantum chaos, which involves the study of classically chaotic systems in the quantum regime, first requires a faithful representation of it's classical time evolution. In

the case of two-dimensional area preserving maps, this is given by a *quantum map* that is unitary, popularly termed the *Floquet operator*. The *quantization* of any general two-dimensional map is not immediately clear. Commonly, quantum maps are one of either two kinds, quantizations of 1.5 DOF systems, mostly *kicked* Hamiltonian systems or quantizations of abstract maps like the baker and cat map. Most of the studies in quantum maps are restricted to 2-dimensional area preserving maps, because of it's simplicity. In the case of *kicked* Hamiltonian systems we have a general template to find the *Floquet* operator. The Hamiltonian has the following structure and as is the case with any quantum state, time evolution is given by solving the Schrödinger equation.

$$H = H_0 + V \sum_{n=-\infty}^{\infty} \delta(t/T - n) \tag{2.8}$$

$$\iota\hbar \frac{\partial}{\partial t}|\psi\rangle = H_0|\psi\rangle + V\delta_T(t)|\psi\rangle \tag{2.9}$$

By following a procedure similar to the case of finding the classical mapping for *kicked* Hamiltonian systems, the corresponding *Floquet* operator can be derived. First we start with a state $|\psi(n)\rangle$, immediately after the $n'th$ kick. Once again, the Hamiltonian H, is just H_0 between two successive kicks, and the corresponding time evolution operator is just $e^{-\frac{i}{\hbar}H_0T}$. The potential term is later integrated over the kick to give the final state $|\psi(n+1)\rangle$.

$$|\psi(n+1)\rangle = \exp(-\frac{i}{\hbar}VT)\exp(-\frac{i}{\hbar}H_0T)|\psi(n)\rangle \tag{2.10}$$

2.4.1 Quantum kinematics on the torus

In this thesis, since we are primarily interested in studying 2-dimensional area-preserving maps, we have restricted the phase space to a compact torus topology by using modulo 1 operations on both q and p. It is important to note that the unit torus topology is not natural to the baker map, since the points $(0,0)$ and $(1,1)$ are equivalent, although they are two different fixed points of the system. This is tackled by a tricky use of phases, which will be discussed when the baker map is quantized subsequently.

Quantum mechanics on the torus is accomplished by dividing the phase space into N cells each of area $2\pi\hbar$, i.e $N = 1/h$. The value of N is finite and is the dimensionality

of the Hilbert space, with h called the scaled Planck's constant. The N eigenstates of the position and momentum are labeled as, $|q_n\rangle$ and $|p_m\rangle$ with eigenvalues $q_n = n/N$ and $p_m = m/N$, respectively [11]. The labeling of the eigenstates is done periodically but for an overall phase, i.e $|q_n + N\rangle = e^{2\pi i\alpha}|q_n\rangle$ and $|p_m + N\rangle = e^{2\pi i\beta}|p_m\rangle$. Therefore, quantization on the torus provides us with the freedom to choose two arbitrary phases. The transformation function between the position and momentum eigenstates is given by the *discrete-Fourier transform* on N sites, G_N. The Fourier transform, G_N is dependent on the phases, α and β, and is an $N \times N$ unitary matrix with the matrix elements defined as,

$$(G_N)_{nm} = \langle q_n|p_m\rangle = \frac{1}{\sqrt{N}} \exp(-2\pi i(n+\alpha)(m+\beta)/N) \tag{2.11}$$

The position and momentum translation operators, U and V are defined as,

$$\langle n|U = \langle n+1| \ ; \ V|m\rangle = |m+1\rangle \tag{2.12}$$

$$U^N = e^{2\pi i\alpha} \ ; \ V^N = e^{2\pi i\beta} \tag{2.13}$$

It is easy to verify that the momentum and position states are eigenvectors of U and V respectively. Consequently, the commutation relation between U and V can be derived to be, $UV = VUe^{-2\pi i/N}$.

2.4.2 Quantum standard map

In the case of the standard map with a unit time period between successive kicks, $H_0 = \frac{1}{2}\hat{p}^2$ and $V = -\frac{k}{4\pi^2}\cos(2\pi\hat{q})$ and the corresponding *Floquet operator* in the position representation is given by,

$$U_{mn} = \langle q_m|U|q_n\rangle = \langle q_m|e^{\left(\frac{i}{\hbar}\frac{k}{4\pi^2}\cos(2\pi\hat{q})\right)}e^{\left(-\frac{i}{2\hbar}\hat{p}^2\right)}|q_n\rangle \tag{2.14}$$

$$U_{mn} = \frac{1}{N}e^{\left(\frac{iNk}{2\pi}\cos(2\pi\frac{n+\alpha}{N})\right)}\sum_{j=0}^{N-1} e^{\left(-\frac{i\pi(j+\beta)^2}{N}\right)}e^{2\pi i(m+\beta)(n-m)/N} \tag{2.15}$$

where the second expression is derived by introducing two complete set of momentum basis states on both sides of the kinetic term and making use of the transformation function between the position and momentum basis. Using $\beta = 0$ and performing a

Gaussian sum, the analytical expression for the matrix elements of U become,

$$U_{mn} = \frac{e^{i\pi/4}}{\sqrt{N}} e^{\frac{iNk}{2\pi}\cos\left(2\pi\left(\frac{m+\alpha}{N}\right)\right)} e^{i\pi(m-n)^2/N} \tag{2.16}$$

The value of $\beta = 0$ corresponds to periodic boundary conditions and $\beta = 1/2$ corresponds to anti-periodic boundary conditions. For other values of β the quantum standard map has been shown to break time-reversal symmetry in ref. [29]. A similar role is played by α for the case of parity-symmetry. Thus for our case, the quantum map has time-reversal symmetry.

2.4.3 Quantum baker map

The baker map was first quantized by Balazs and Voros in 1989 [11] and later modified by Saraceno [12]. There is a lot of literature on various quantization schemes, but for the purpose of this thesis, we will refer to the Balazs-Voros-Saraceno quantization. The idea behind the quantization is that the Floquet operator must possess all the symmetries of the classical map and give back the correct transformation in the classical limit. The quantization is carried out by defining the action of the baker map geometrically (refer fig1.2) on the Hilbert space by analogously defining orthogonal subspaces. The resulting Floquet operator has a very simple block diagonal structure in terms of the *discrete-Fourier transform*, G_N (see eqn.2.11).

$$U_N = G_N^\dagger \begin{pmatrix} G_{N/2} & 0 \\ 0 & G_{N/2} \end{pmatrix} \tag{2.17}$$

The quantization proposed by Balazs and Voros (B-V), had a periodic boundary conditions, i.e $\alpha = 0 = \beta$. This was later modified by Saraceno to have an anti-periodic boundary condition, i.e $\alpha = 1/2 = \beta$. This was observed to restore the reflection symmetry in the quantum map. One simple motivation to use an anti-periodic boundary condition is the equality of the points $(0, 0)$ and $(1, 1)$ on the torus, both of which are distinct fixed points of the baker map. This is remedied in the quantum version by the additional phase distinguishing both the points.

As discussed in the previous chapter, the baker map has two fundamental symmetries, *reflection* and *time-reversal* symmetry. The latter being an anti-canonical symmetry, the quantum mechanical equivalent has to be an anti-unitary symme-

try. The time-reversal operator is G_N and the anti-unitary symmetry is given by, $G_N U G_N^{-1} = (U^{-1})^*$. The quantum reflection operator, R_N acting on the position eigenstates is, $R_N|q_n\rangle = |q_{N-n-1}\rangle$. Therefore, the matrix elements of the reflection operator in the position basis is given by $(R_N)_{nm} = \delta(N-n-m-1)$. It is easy to verify that $R_N = -G_N^2$ and $R_N U R_N = U$. The nearest-neighbor-spacing (NNS) of eigenangles of the quantum baker map has been known to closely resemble a *Gaussian orthogonal ensemble*(GOE), as expected of systems with no time-reversal invariance [11, 12].

2.4.4 The three-baker map

The quantization of this map is a straightforward extension of the quantum baker map. In presenting the classical map, it was mentioned that the baker in A and B are disjoint and commute with each other. The analogous property would be to assume that A and B are quantum bakers acting on two disjoint Hilbert spaces without any interaction between them. This would result in a block-diagonal structure for the quantum map B_{AB}. However, quantizing A and B as quantum maps acting on disjoint Hilbert spaces does not entail the possibility of *tunneling* between A and B, which is to be expected. Therefore, the quantum map of the bakers in A and B is given by,

$$\tilde{B}_{AB} = G_N^\dagger \begin{pmatrix} G^L_{N/2} & 0 & G^R_{N/2} & 0 \\ 0 & G^L_{N/2} & 0 & G^R_{N/2} \end{pmatrix} \tag{2.18}$$

$$G_{N/2} = \begin{pmatrix} G^L_{N/2} & G^R_{N/2} \end{pmatrix} \tag{2.19}$$

where G_N is the discrete-Fourier transform on N sites (eqn.2.11). We have just mentioned the quantum map here, but for the detailed procedure of the quantization, please refer to reference [17]. In the same article, it was shown that tunneling between A and B was indeed a crucial feature that did have manifestations on the quantum relaxation. In particular, it was shown that the quantum relaxation with tunneling was faster than the classical relaxation for initial time. The baker map on C can be quantized by a straightforward application of the quantum baker map presented in the previous section. Let us denote the quantum baker map acting on k sites as U_k. In this case, we have the baker in C acting on $2N\alpha$ sites. Let us denote the quantum baker map on C as B_α where α is the parameter that defines the boundary of C and

$U_{2N\alpha}$ is the quantum baker map acting on $2N\alpha$ sites.

$$\tilde{B}_\alpha = \begin{pmatrix} I_{N(1/2-\alpha)} & 0 & 0 \\ 0 & U_{2N\alpha} & 0 \\ 0 & 0 & I_{N(1/2-\alpha)} \end{pmatrix} \tag{2.20}$$

The quantum three-baker map thus becomes, $U_{three-baker} = \tilde{B}_\alpha \tilde{B}_{AB}$.

2.4.5 The lazy-baker map

The lazy-baker as mentioned earlier in the chapter, belong to a class of maps that are non-uniformly hyperbolic with disparate actions of stretching on one half and geometrical transformation on the other. The quantization of the SRS and SR maps were presented by Lakshminarayan in [18]. Once again, we just briefly mention the important features of the quantization. The quantization of the SR map that we are interested in is a special case of the SRS map described in the above mentioned reference. The SRS map has three partitions with the usual stretching and folding in the first and the third with a rotation by $\pi/2$ of the second. The quantization of these maps is achieved by partitioning the Hilbert space into disjoint subspaces with the corresponding quantum actions in the respective spaces. However, the SR map with it's disparate dynamics on the boundary is not a natural candidate for quantization on a torus. Therefore, the quantization has been performed with a thin strip of stretching partition to account for this. Classically, this is identical to an SRS map with an infinitesimal third partition.

$$U_{lazy-baker} = G_N^\dagger \begin{pmatrix} G_{N/2} & 0 & 0 \\ 0 & I_{N/2-1} & 0 \\ 0 & 0 & i \end{pmatrix} \tag{2.21}$$

Where G_N is once again the discrete-Fourier transform on N sites and $I_{N/2-1}$ is the identity matrix of dimension $(N/2-1) \times (N/2-1)$.

2.5 Quantum relaxation

The quantum equivalent of the classical correlation function is derived by the use of projectors in Hilbert space as the analogous entities to the classical characteris-

tic functions. Just as in classical case, we define two *orthogonal* subspaces A and B in the Hilbert space and their corresponding projectors $\hat{P}_A$ and $\hat{P}_B$. The time evolution of the projector $\hat{P}_A$ is given by $\hat{P}_A(t) = U\hat{P}_A U^\dagger$, where U is the Floquet operator. Naturally, $\hat{P}_A(t)\hat{P}_B$ is the projection of the time evolved subspace A onto B. We make the quantum-classical correspondence using coherent states defined on the torus. Coherent states, as the name suggests are minimal uncertainty states on the torus. There is a lot of literature on ways to define a coherent state on the torus, but for the purpose of this section the specific details of the construction are irrelevant. However, we refer to the prescription of Saraceno [12]. In essence, the phase space representations of coherent states are localized at specific phase space points with a defined uniform uncertainty in both position and momentum, denoted by $|p, q\rangle$. The phase space representations are the quantum analogue of the classical probability distribution on the phase space. Wigner and Husimi distributions are the popular choices for such a phase space representation. We will use the latter for their non-negative property. Wigner and Husimi representations in continuous quantum mechanics has been described in detail in ref. [30]. Saraceno in [12] discusses using a similar construction for the Husimi representation on the torus. Given any operator $\hat{P}$, the Husimi distribution W_h is defined as,

$$W_h(q, p) = \langle p, q|\hat{P}|p, q\rangle \tag{2.22}$$

We now ask what happens to the integral of the Husimi representation of a coherent state over all position and momentum. Having defined the coherent states as minimum uncertainty states in phase space,Naturally, we expect the integral to be the area of the uncertainty in phase space

$$\int\int \langle p, q|p_0, q_0\rangle\langle p_0, q_0|p, q\rangle dpdp = h \tag{2.23}$$

We normalize this expression by a simple rescaling of the infinitesimal area to reflect the coherent states as a complete set and calculate the integral of the Husimi representation of a projector, P_A (let) over the phase space. Making use of the classical analogy of the projectors, we expect the integral to give us the measure of the corresponding subset, A in phase space. However, the integral of a phase space representation over the phase space is also analytically equal to the trace of the concerned

operator. [30]

$$\langle p, q|\hat{P}_A|p, q\rangle \equiv \chi_A \tag{2.24}$$

$$\int\int \langle p, q|\hat{P}_A|p, q\rangle \ \frac{1}{h} dpdq = \mathrm{Tr}(\hat{P}_A) = \frac{1}{h}\mu(A) \tag{2.25}$$

Using the above equation along with the fact that the rescaled Planck's constant $h = 1/N$, we can calculate the quantum correlation between two projectors, as a function of time using a one-to-one correspondence with the classical correlation using the above derived equalities.

$$\mu\left(f^t A \cap B\right) = h \cdot \mathrm{Tr}(U^t \hat{P}_A U^{-t} \hat{P}_B) \tag{2.26}$$

$$\boxed{c(t) = \frac{N}{\mathrm{Tr}(\hat{P}_A)\,\mathrm{Tr}(\hat{P}_B)}\,\mathrm{Tr}(U^t \hat{P}_A U^{-t} \hat{P}_B)} \tag{2.27}$$

Now, we can quantify the quantum mixing between any two subspaces of the Hilbert spaces using the quantum correlation, $c(t)$. It is only natural to expect that the correlation relaxes to 1, since we have built the expression for $c(t)$ using an analogy between the classical and quantum expressions. In the result section, we find that it does indeed approach 1 with time. In the classical case, for ease of use we had defined A and B to be the left and right halves of the classical phase space, therefore we first study the case when $\hat{P}_A$ and $\hat{P}_B$ are the analogous orthogonal projectors.

$$\hat{P}_A = \sum_{i=0}^{N/2-1} |q_i\rangle\langle q_i| \ \&\ \hat{P}_B = \mathbb{1}_N - \hat{P}_A \tag{2.28}$$

$$\implies \mathrm{Tr}(\hat{P}_A) = \mathrm{Tr}(\hat{P}_B) = \frac{N}{2} \tag{2.29}$$

Let us denote these special projectors as $\hat{P}_1$ and $\hat{P}_2$ respectively. In the results chapter, we have also calculated the relaxation when the subspaces A and B are not exhaustive or orthogonal, and we infer that it does not seem to be affect the relaxation profile in the case of the lazy-baker.

2.6 Random unitary transformation

Having quantified "mixing" in Hilbert space, the motivation was to find if there existed an analogue of the R-P resonances in the quantum regime. Therefore, the idea is to study the relaxation between two initially disjoint "*random projectors*" in Hilbert space. So far, there has been some degree of arbitrariness in defining the subsets/subspaces to calculate the relaxation, although there is nothing special about the choices classically. The R-P resonances are characteristics of a given system that have no bearing on the structure of the partitions A and B. Therefore, we investigate what happens to the relaxation when the projectors are "random", i.e there is no intuitive way to decipher their classical analogues. At this juncture, we address two natural questions, 1) How do we create a random projector and 2) Can we quantify it's "*randomness*"?.

We create a random projector by making use of random unitary transformations acting on the usual projectors. Random unitary transformations can be viewed as a rotation in Hilbert space, since it is "trace-preserving". Given a projector $\hat{P}_A$, we describe the randomized projector to be, $V\hat{P}_A V^\dagger$, where V is a unitary matrix chosen from the set of all unitary based on the *Haar* measure. Before we define how to generate the unitary matrix, it is essential to describe the *Haar* measure. Let us denote the set of all $N \times N$ unitary matrices to be $U(N)$. Additionally, the set $U(N)$ is said to be compact Lie group. In the context of this thesis, we define the *Haar* measure of $U(N)$ as a "unique" measure, μ over $U(N)$ that is invariant under group multiplication, i.e

$$\mu(S) = \mu(gS) = \mu(Sg) \;\forall\; S \subset U(N),\; g \in U(N) \tag{2.30}$$

For a more rigorous definition of the *Haar* measure in the broad context of compact topological groups, please refer to article [31]. The *Haar*, defined as a probability measure, i.e $\mu(U(N)) = 1$, in simple terms can be viewed as the analogue of a uniform probability distribution over a closed set. The set of all unitary matrices with the above defined Haar measure on the unitary group, $U(N)$ belong to the *circular unitary ensemble*(CUE), introduced by Dyson. Generating matrices belonging to the CUE, numerically was discussed by Życzkowski and Kus [32]. However, we refer to a more recent article by Mezzadri [33] to generate such unitary matrices. The algorithm used has just been mentioned in brief, without going into any detail.

1. Generate a matrix Z, whose elements are complex numbers with real and imaginary parts as $i.i.d$ standard normal random variables.

2. Perform a standard QR decomposition of Z, available in almost all linear algebra packages. $Z = QR$.

3. Define a diagonal matrix D, whose diagonal entries are the diagonal entries of the matrix R normalized to unit norm. $D_{jj} = \frac{R_{jj}}{|R_{jj}|}$

4. Now the matrix $Q' = QD$. is a unitary matrix distributed with the Haar measure.

Having generated a random unitary matrix, the projector $V\hat{P}_A V^\dagger$ becomes a random projector. Now to tackle the question of quantifying it's "randomness", we first need a reference with respect to which we can compare. In this case, the reference is the original projector $\hat{P}_A$, or in other words, $V = \mathbb{1}$. We use the *Frobenius* or the *Hilbert-Schmidt* norm between V and the identity matrix as a measure of the degree of randomness. In order to gain a analytical expression for the norm, we use a particular structure for V instead of it simply belonging to the CUE.

$$V = v \cdot U_d^\epsilon \cdot v^\dagger,\ v \in CUE \tag{2.31}$$

$$(U_d^\epsilon)_{jk} = \delta_{jk} \exp\left(i\epsilon\theta_j\right) \tag{2.32}$$

where the θ_j's are sampled uniformly from $[-\pi, \pi]$. We can now analytically find an expression for the Frobenius norm between identity and V.

$$||I - V||^2 = \mathrm{Tr}((I - V)(I^\dagger - V^\dagger)) = 2N - 2Re(\mathrm{Tr}(V)) \tag{2.33}$$

$$= 2N\left(1 - \frac{1}{N}\sum_{n=0}^{N-1} e^{(i\epsilon\theta_n)}\right) = 2N\left(1 - \langle e^{(i\epsilon\theta_n)}\rangle\right) \tag{2.34}$$

$$= 2N\left(1 - \frac{\sin(\pi\epsilon)}{(\pi\epsilon)}\right) \tag{2.35}$$

$$\implies ||I - V||^2 = \frac{N\epsilon^2\pi^2}{3} = \frac{(\tilde{\epsilon})^2\pi^2}{3}\ ;\ \tilde{\epsilon} = \frac{\epsilon}{\sqrt{N}} \tag{2.36}$$

Replacing ϵ with $\tilde{\epsilon}$, we can make the norm independent of the dimensionality. However, in the process of redefining V, we have essentially modified the random unitary matrix. From eqn.2.31, it is clear that U_d^ϵ are the eigenvalues of the matrix V and

this implies that the random unitary transformations are such that it's eigenvectors have the property of CUE, but it's eigenvalues do not. Nevertheless, we do not find any significant effect of this in the relaxation behavior. The expression for relaxation remains the same, with only the projectors replaced by new "random" ones.

2.7 Relaxation averaged over the Haar measure

Motivated by studies of averages of relaxation [26,34], which seem to show distinctly different properties when the classical limit is chaotic and regular, we study the relaxation of random projectors averaged over the CUE. Moreover, ensemble averages in studies of quantum chaos are somewhat of a commonality and have been known to come up with universal properties.

$$\langle C_q(t)\rangle_{cue} = \frac{N}{\mathrm{Tr}(\hat{P}_A)\,\mathrm{Tr}(\hat{P}_B)}\langle \mathrm{Tr}(U^t(V\hat{P}_AV^\dagger)U^{-t}(V\hat{P}_BV^\dagger))\rangle_{CUE} \tag{2.37}$$

where the matrix V is as defined in eqn. 2.31.

Averages over specific ensembles of random matrices have been a important part of studies in random matrix theory(RMT) and quantum chaos. In our case, since we have used unitary matrices from the CUE, we require an average over the Haar measure. For the sake of simplicity, let us represent the pre-factor all together with a single constant character η. Inserting complete sets of position eigenkets $|q_j\rangle$ between all the matrices, we get

$$\eta\langle \sum_{x_1\ldots x_8=0}^{N-1} (U^t_{x_1x_2}V_{x_2x_3}(\hat{P}_A)_{x_3x_4}V^*_{x_5x_4}U^{-t}_{x_5x_6}V_{x_6x_7}(\hat{P}_B)_{x_7x_8}V^*_{x_1x_8})\rangle \tag{2.38}$$

$$\implies \eta \sum_{x_1\ldots x_8=0}^{N-1} (U^t_{x_1x_2}(\hat{P}_A)_{x_3x_4}U^{-t}_{x_5x_6}(\hat{P}_B)_{x_7x_8})\ \langle V_{x_2x_3}V^*_{x_5x_4}V_{x_6x_7}V^*_{x_1x_8}\rangle \tag{2.39}$$

Averages of such types of expressions as in eqn. 2.39 have been called moments of $U(N)$. Such types of averages over the Haar measure, has been studied in an article by Puchala and Miszczak [35]. In fact, an exact analytical expression for the case we

are interested in has also been mentioned in the same article using which,

$$\langle V_{x_2x_3}V_{x_6x_7}V^*_{x_5x_4}V^*_{x_1x_8}\rangle_{CUE} = \frac{(\delta_{x_2x_5}\delta_{x_3x_4}\delta_{x_6x_1}\delta_{x_7x_8}) + (\delta_{x_2x_1}\delta_{x_3x_8}\delta_{x_6x_5}\delta_{x_7x_4})}{N^2-1} \tag{2.40}$$

$$- \frac{(\delta_{x_2x_5}\delta_{x_3x_8}\delta_{x_6x_1}\delta_{x_7x_4}) + (\delta_{x_2x_1}\delta_{x_3x_4}\delta_{x_6x_5}\delta_{x_7x_8})}{N(N^2-1)} \tag{2.41}$$

Using the above expression, we can derive an analytical expression for the relaxation, $C_q(t)$ averaged over the CUE.

$$\langle C_q(t)\rangle_{cue} = \frac{1}{N^2-1}\left[\left[N^2 - |\operatorname{Tr}(U^t)|^2\right] + \frac{\operatorname{Tr}(\hat{P}_A\hat{P}_B)N}{\operatorname{Tr}(\hat{P}_A)\operatorname{Tr}(\hat{P}_B)}\left[|\operatorname{Tr}(U^t)|^2 - 1\right]\right] \tag{2.42}$$

If we assume that the initial projectors are orthogonal, then $\operatorname{Tr}(\hat{P}_A\hat{P}_B) = 0$. In such a situation, the expression for the averaged relaxation becomes much simpler, and we consequently find an expression for the fluctuations of the average from the equilibrium value.

$$\boxed{1 - \langle C_q(t)\rangle_{cue} = \frac{1}{N^2-1}\left[|\operatorname{Tr}(U^t)|^2 - 1\right]} \tag{2.43}$$

We immediately see that if the projectors are initially orthogonal, there is no dependence of the average on the subspaces A and B. The term $|\operatorname{Tr}(U^t)|^2$ is a well studied quantity termed the "*spectral form-factor*" [36, 37], but for a constant prefactor of $1/N$. In random matrix theory, the spectral form-factor, is defined as the Fourier transform, $\kappa(t)$ of the two-level correlation in the spectrum. Semiclassical studies of the spectral form-factor have elucidated the behavior of κ over different random matrix ensembles [4, 38]. For the CUE this has a particularly simple structure as follows.

$$\kappa_N(t) = \frac{1}{N}\langle|\operatorname{Tr}(U^t)|^2\rangle_{cue} = \begin{cases} N, & t = 0 \\ \frac{|t|}{N}, & 0 < |t| \leq N \\ 1, & |t| > N \end{cases} \tag{2.44}$$

The variable t can be replaced by a normalized time $\tau = \frac{t}{T_H}$, where $T_H = 2\pi\hbar$ is known as the Heisenberg time. When the concerned random matrix ensemble is

COE, the form-factor has the following structure [39].

$$\kappa_N(\tau)_{coe} = \begin{cases} N, & \tau = 0 \\ (2\tau - \tau \ln(1+2\tau)), & 0 < \tau < 1 \\ 2 - \tau \ln\left(\frac{2\tau+1}{2\tau-1}\right), & \tau \geq 1 \end{cases} \tag{2.45}$$

Although the particular structure of the form-factor is different for the CUE and COE, the asymptotic limit is the same for both, i.e $|\operatorname{Tr}(U^t)|^2$ tends to the value of N for large t. When $t = 0$, $|\operatorname{Tr}(U^t)|^2 = N^2$, and the relaxation fluctuation average is 1, which is obvious since $\operatorname{Tr}(\hat{P}_A\hat{P}_B) = 0$ and when $t > N$, it is $1/(N+1)$, which in the semiclassical limit approaches 0. Thus, our boundary conditions seem to be satisfied. However, note that although the Floquet operator, U does indeed belong to COE or CUE, the spectral form-factor is not self-averaging [37], and therefore, it's numerical behavior is hardly smooth as described above. What is interesting to note is that, we observe a saturation of the average relaxation to a value significantly lower than 1. What this signifies, is a lack of complete mixing between two initially orthogonal subspaces in Hilbert space. This value approaches 1 in the semiclassical limit, as we should expect since the classical relaxations approach 1. A calculation of the standard deviation of this relaxation fluctuations can be made using the same technique explained in [35]. However, an analytical expression for the standard deviation would be more involved, and we have not done the same due to lack of time. Nevertheless, the standard deviation of the fluctuations must also approach zero in the semiclassical limit. A similar study of the time average of the relaxation in the case of bounded chaotic systems by Lakshminarayan [26], calculate the standard deviation of the time averaged relaxation fluctuations to have a power law dependence on N.

2.8 Numerical calculation

All numerical calculation presented in this thesis have been done in C++ programming language. In particular all linear algebra calculations have been done using the open-source linear algebra package for C++, "*Armadillo*" [40]. Most of the graphs have been plotted using the software, "*Gnuplot*" [41]. A few of the graphs, in particular 3D surface plots have been made using the commercial software "*Mathematica*".

Chapter 3

Results and Discussion

3.1 Relaxation of the lazy-baker

We present results of numerical calculation of the quantum relaxation, $c(t)$ when the projectors A and B have a clear classical analogue and compare it with the corresponding classical relaxation law derived analytically.

1. When A and B are chosen to be the left and right halves of the phase space, we had calculated an expression for the relaxation law, given by eqn.2.7. The quantum projectors in this case is given by eqn.2.28. We will use the representation $\hat{P}_1$ and $\hat{P}_2$ for these projectors.

From the fig.3.1 and 3.2 we see that there is indeed a quantum-classical correspondence in the relaxation profile. We observe that the quantum relaxation behaves exactly like the classical law for initial time, till the classical system has relaxed to equilibrium. Although the classical systems has relaxed, there are fluctuations in the quantum relaxation. The fluctuations of the quantum relaxation about the equilibrium are a purely quantum effect and it is observed to approach zero as N becomes greater. The observations are exactly identical to ones by Lakshminarayan in [17] for the three-baker map.

In the relaxation profile, we observe a peculiar difference in the quantum relaxation of both fig.3.1 and 3.2, when the dimensionality is a power of 2. It has been shown before that powers of 2 are special for the baker map with their eigenstates being proved to be multifractal [42]. We believe that this is the reason for the revival that is observed in the relaxation.

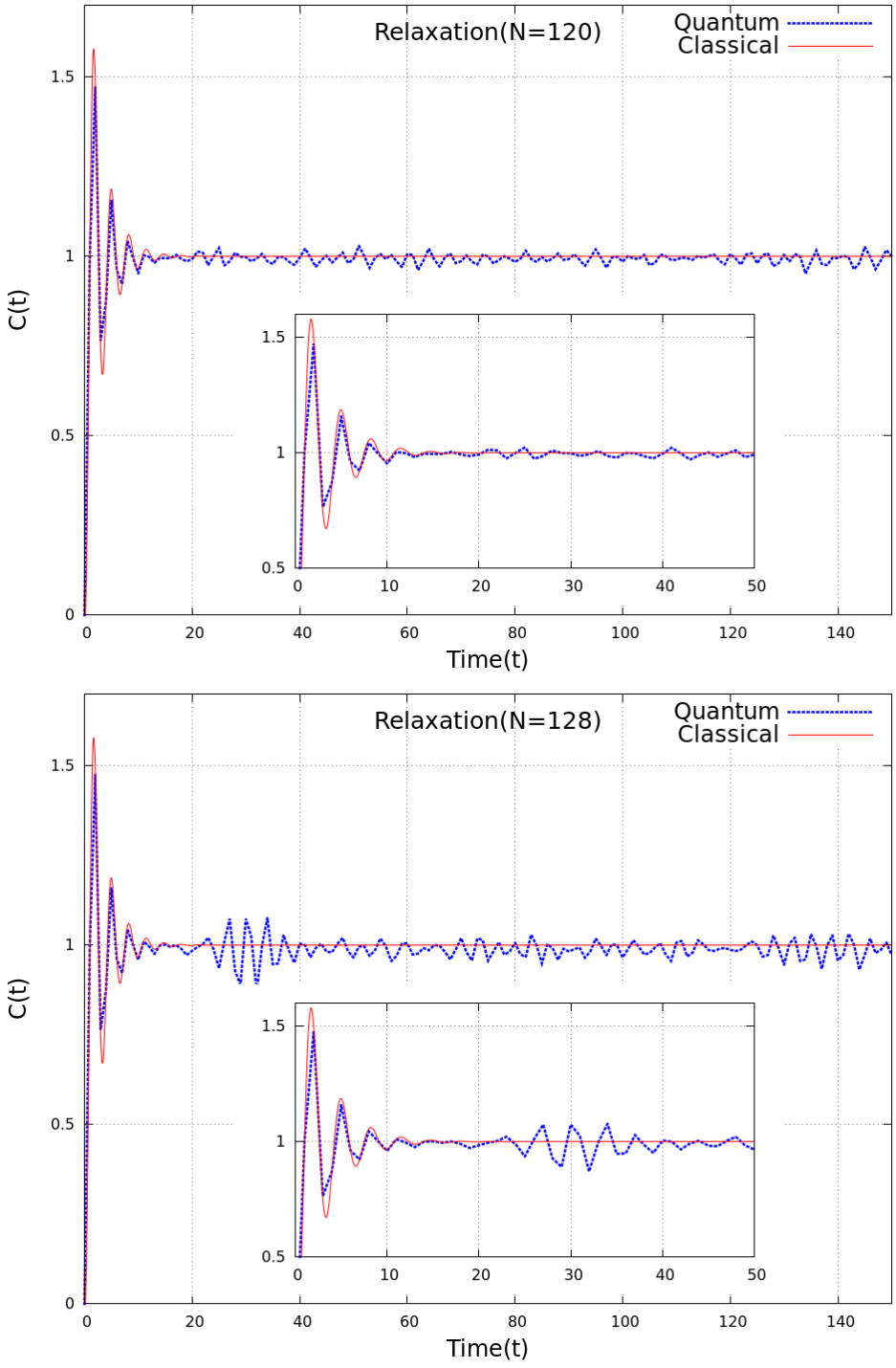

Figure 3.1: A plot of the quantum and classical relaxation of the lazy baker for two values of $N = 120, 128$. The inset shows a magnified view of the same

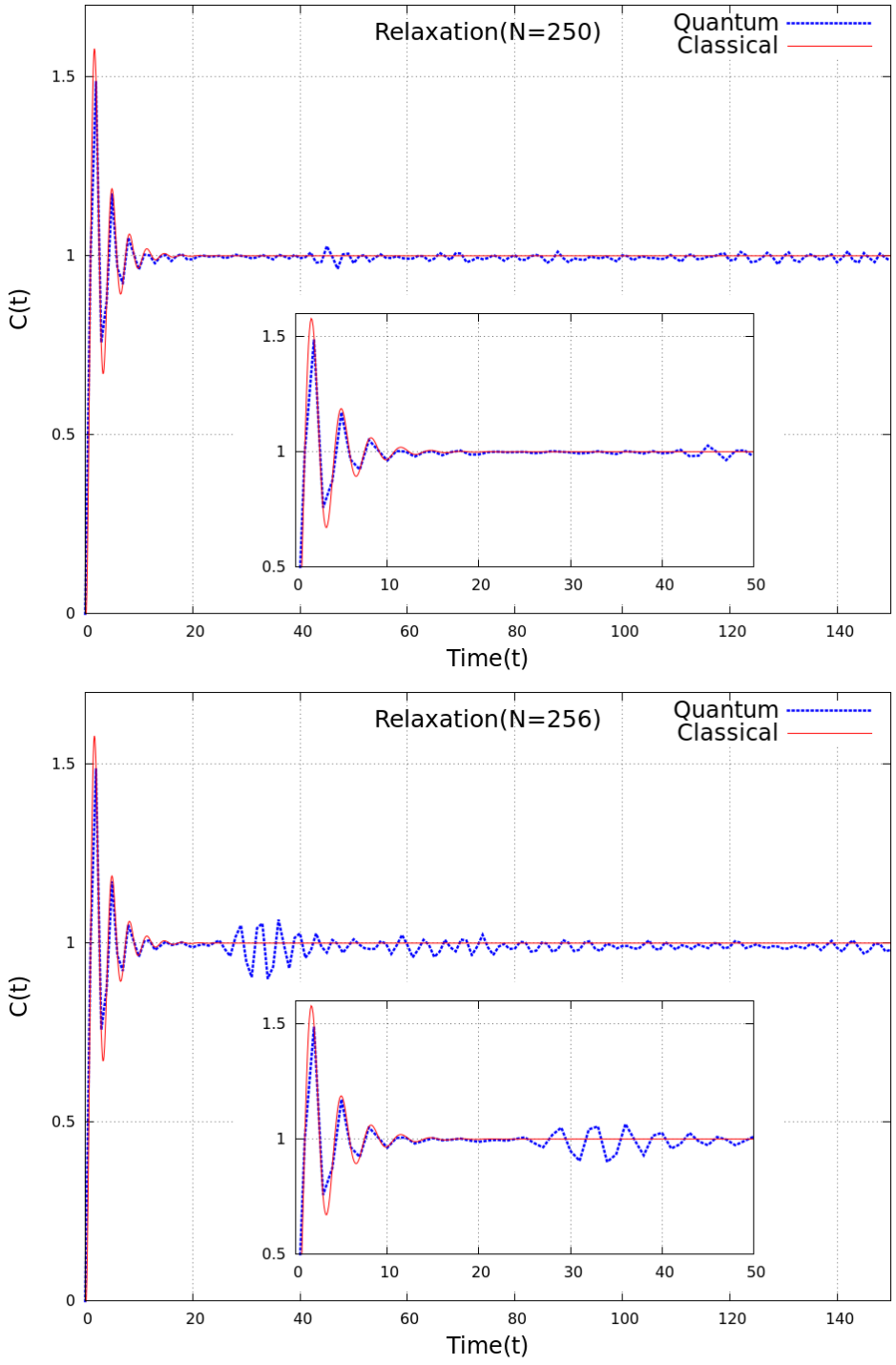

Figure 3.2: Same as fig.3.1 but for $N = 250, 256$

To add further evidence to the quantum-classical correspondence, we calculate the classical relaxation law for two different sets of partitions using the same Markov

partitions.

2. When A and B are the Markov partitions 1 and 3 in fig.2.3, i.e A is the left half and B, the bottom-right quarter of the unit phase space. The corresponding projectors, $\hat{P}_A = \hat{P}_1$ and $\hat{P}_B = \hat{P}_2(G_N^\dagger \hat{P}_1 G_N)$ is the product of the respective position and momentum projectors in position basis, where G_N is the discrete-Fourier transform on N sites 2.11. The classical relaxation law has been derived using the same technique of Markov matrices. It has a similar expression to eqn.2.7 with the term $a = 0.5 + 0.56695i$. The *Ruelle-Pollicott* resonances remain the same, as they are the eigenvalues of the Markov matrix and do not change.

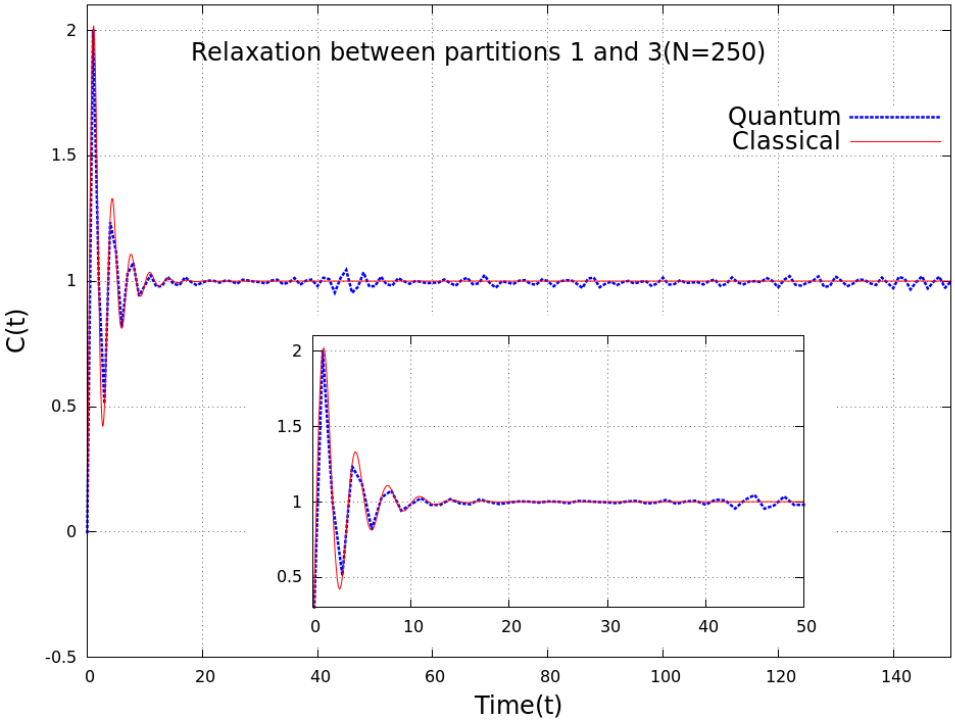

Figure 3.3: Plots of relaxation between the Markov partitions 1 and 3 (fig.2.3), for $N = 250$.

3. When A and B have an overlap. A is the partition 1 plus 2 and B is the partition 2 plus 3. The partition 2 is the overlap and as expected the classical relaxation law is not 0 when $t = 0$. This is also the case with the quantum relaxation as seen in fig.3.4. The value of $a = 0.16667 - 0.18898i$. As with the previous case, the R-P resonances are still the same.

The quantum relaxation does indeed seem to obey the classical law derived. Therefore, from the above results, we can infer that our correspondence between the quan-

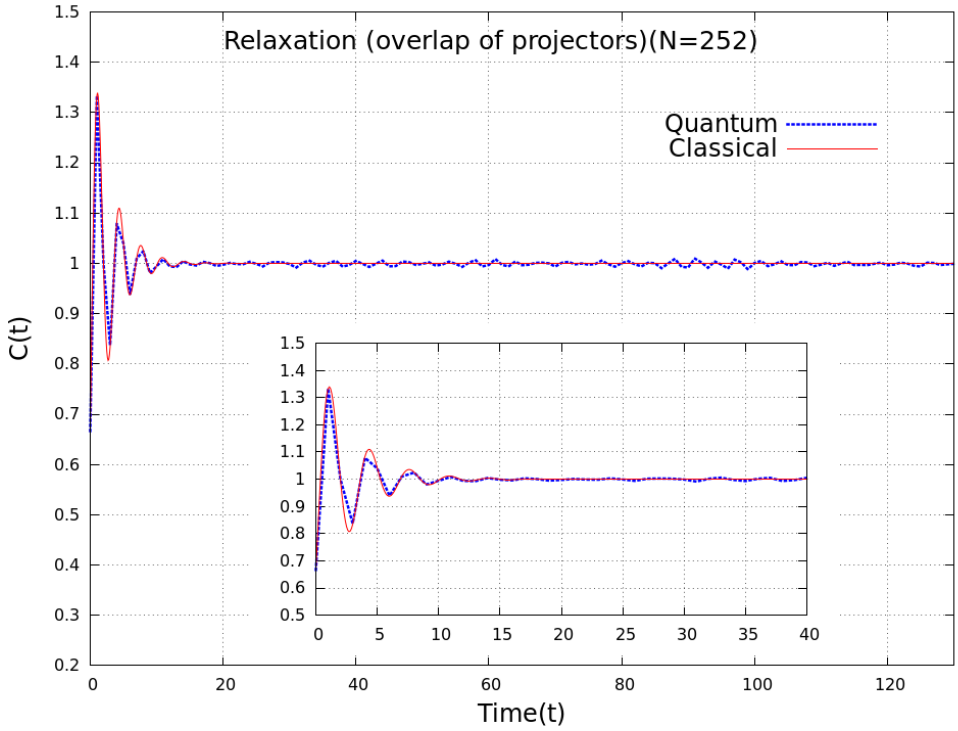

Figure 3.4: Plots of relaxation between the Markov partitions $1+2$ and $2+3$ (fig.2.3), for $N = 252$.

tum and classical relaxation is so far valid even when the partitions are not exactly orthogonal or complete. Moreover, this was one of the primary motivations for us to investigate, if a quantum analogue of the R-P resonances exist.

3.2 Relaxation of random projectors

In this section, we present numerical calculations of relaxation of "random projectors", constructed by a random unitary transformation on simple orthogonal projectors like the once used in the previous section. For the sake of simplicity, we will use the natural left and right half projectors, $\hat{P}_{1,2}$(eqn.2.28) in all cases.

The relaxation of random projectors has been tabulated for both the three-baker (fig.3.5 and 3.6) and lazy-baker (fig.3.7 and 3.8). The random unitary transformation has the structure as in eqn. 2.31 with ϵ quantifying it's "*randomness*". The unitary transformation is $U = VU_d^{\epsilon}V^{\dagger}$, where $V \in CUE$ and $(U_d^{\epsilon})_{jk} = \delta_{jk}\exp(i\epsilon\theta_j)$, with the θ_j's distributed uniformly in $[-\pi, \pi]$. The factor $\epsilon/\sqrt{N}$ is a measure of the normalized

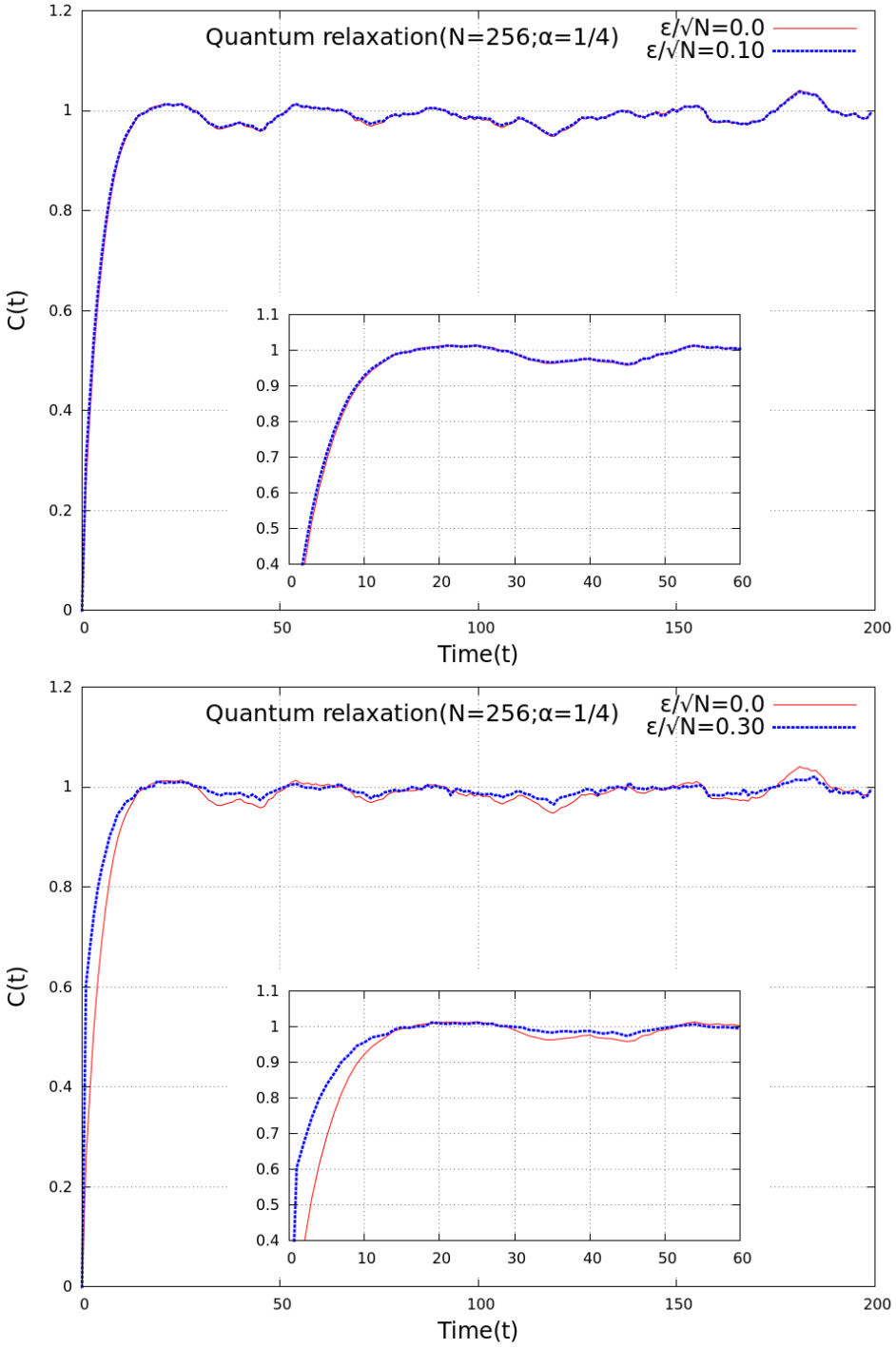

Figure 3.5: Effect of a random unitary transformation of the projectors, on the quantum relaxation, $c(t)$ for the three-baker map. $N = 256$ and $\alpha = 1/4$. $\frac{\epsilon}{\sqrt{N}} = 0.1$ and 0.3

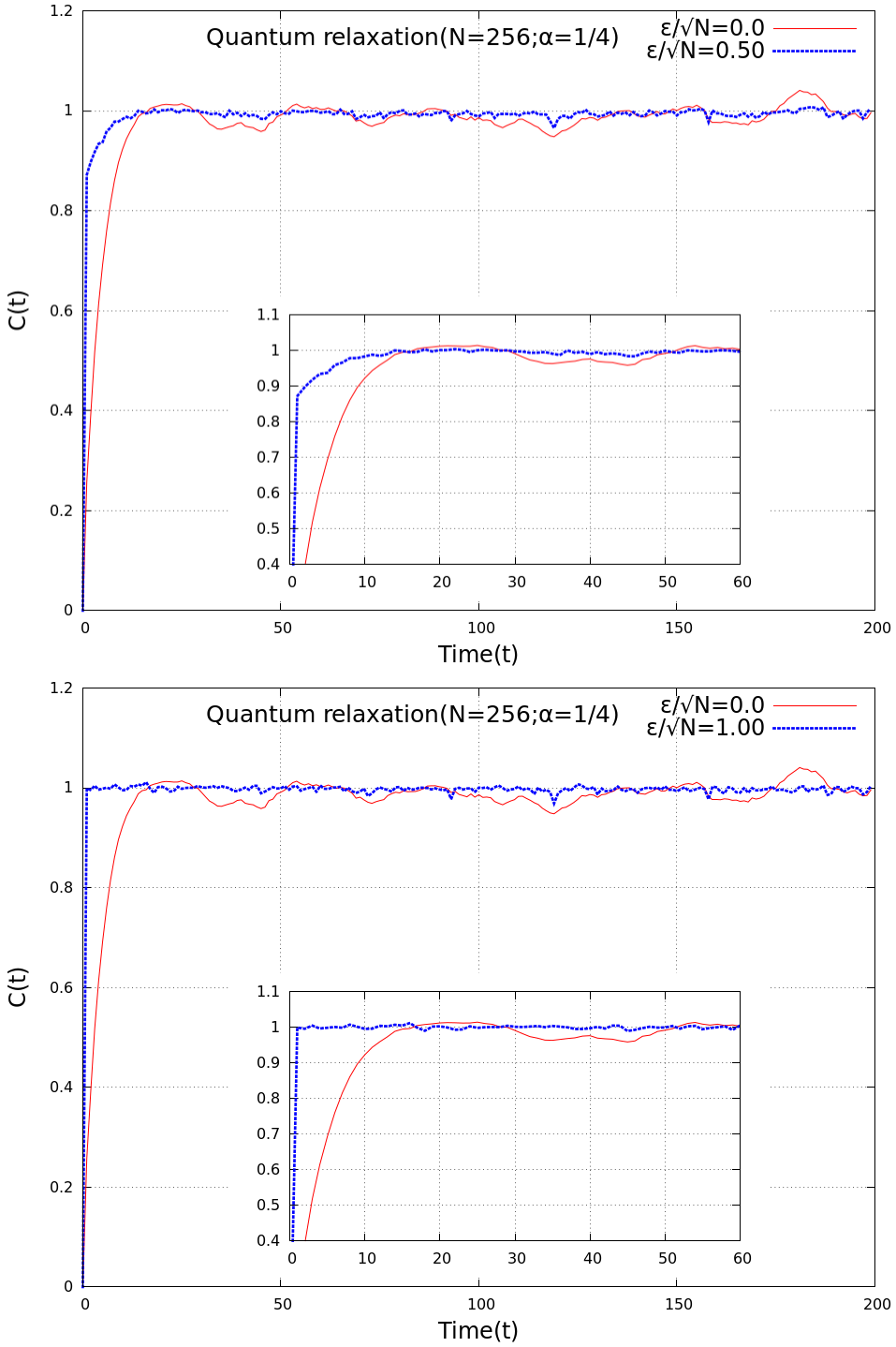

Figure 3.6: Same as fig.3.5 but for $\frac{\epsilon}{\sqrt{N}} = 0.5$ and 1

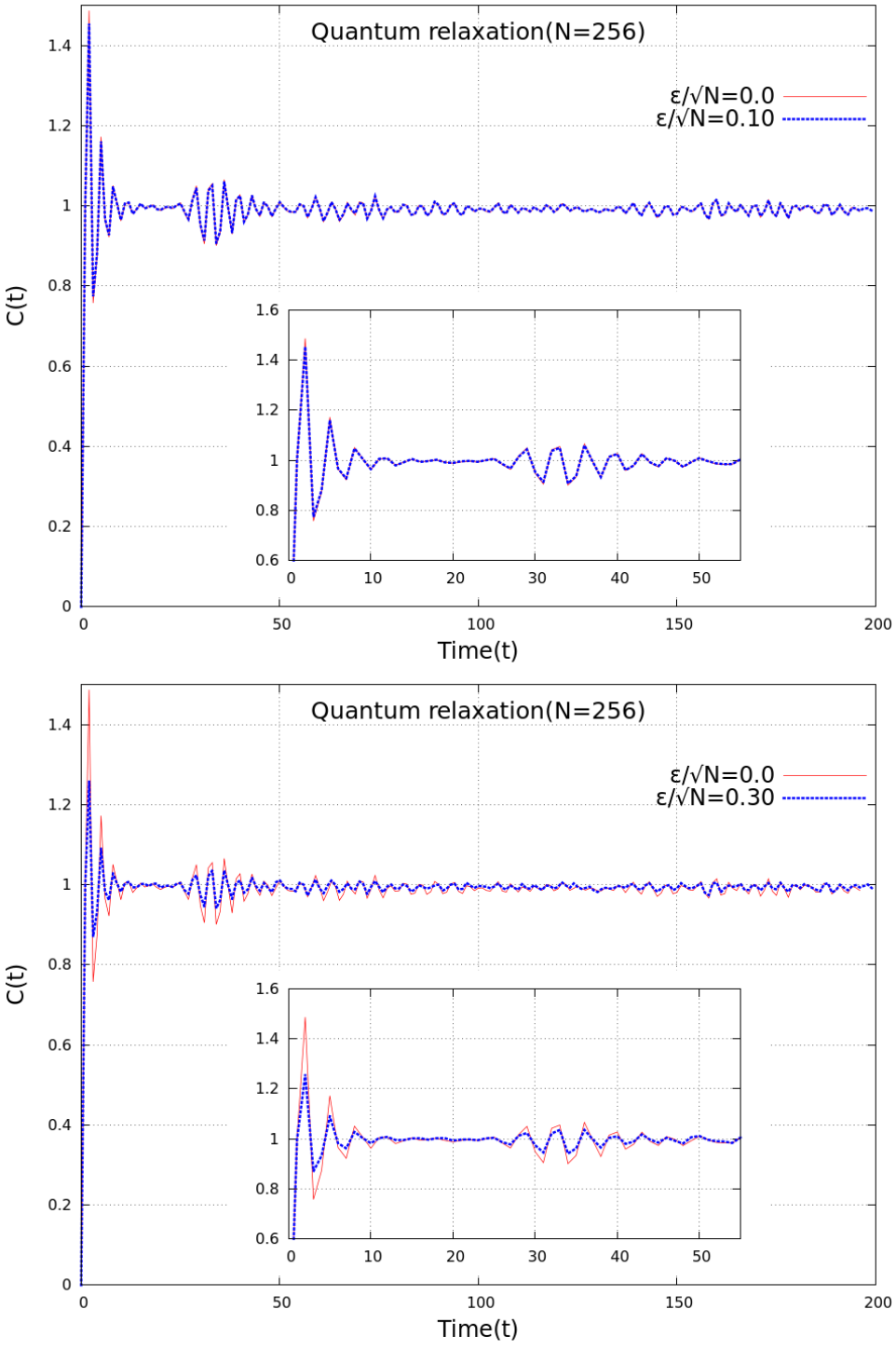

Figure 3.7: Effect of a random unitary transformation of the projectors, on the quantum relaxation, $c(t)$ for the lazy-baker map. $N = 256$. $\frac{\epsilon}{\sqrt{N}} = 0.1$ and 0.3

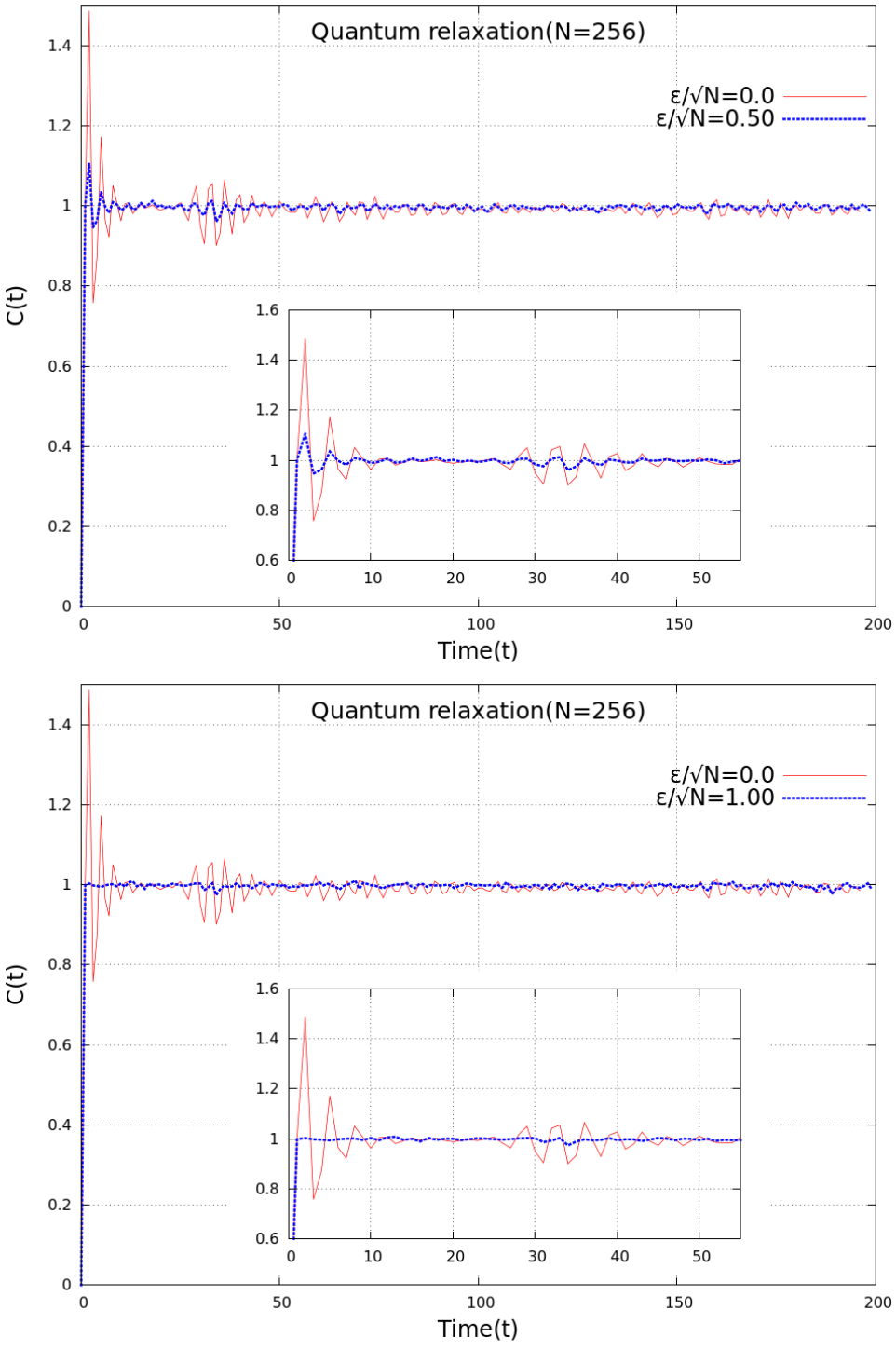

Figure 3.8: Same as fig.3.7 but for $\frac{\epsilon}{\sqrt{N}} = 0.5$ and 1

randomness of the unitary transformation (eqn.2.36). From the corresponding figures we can see that the rate of approach of $c(t)$ to equilibrium becomes greater as the value of ϵ is increased i.e as the transformation becomes more and more random. It is also important to note that all the results in this section are for a single realization of U.

As the value of ϵ is increased, we can see that any signatures of the classical R-P resonances in the quantum relaxation profile is slowly destroyed. When $\frac{\epsilon}{\sqrt{N}}$ is intermediate, the imprint of the R-P resonances are still visible with the characteristic exponential relaxation to equilibrium. For $\frac{\epsilon}{\sqrt{N}} = 0.3$ and 0.5, we can still see a clear effect of the classical R-P resonances. This is the case in both the three-baker and lazy-baker. The above results show us that a random unitary transformation itself entails a *maximal* mixing of the Hilbert space. Subsequently, we show a phase space representation of the random projectors and it becomes clear why there is an immediate relaxation of the system. For the value of $\epsilon/\sqrt{N} = 1$, we can see from eqn.2.31 that the eigenvalues of the unitary transformation will have a complete Poissonian spectrum. As noted in the earlier section, the structure of the unitary transformation used in this study is such that it's eigenvalues are not that of the CUE. Therefore, for the sake of clarity, we also plot the relaxation of random projectors without the special structure, what we can remark as a completely random projector.

We can see from fig.3.9, there is no apparent difference due to the use of the particular structure in eqn.2.31, and there is an immediate relaxation to the equilibrium. As a secondary remark, we also observe that the fluctuations of the relaxation about the equilibrium have also significantly reduced in magnitude, under a random unitary transformation. What is also interesting to note is that under a random unitary transformation of the projector, the observed revival in relaxation of systems with a 2^d dimensionality also approaches zero. These observations entail the question, is there a fundamental difference in the action of the Floquet operator as a result of the random unitary transformation.

We will now plot the phase space representations of the projector $\hat{P}_1$ (eqn.2.28), the classical left half of phase space, under the random unitary transformation (2.31). From the Husimi plots of the "left" projector, we can see the transition of the projector from being confined uniformly to the left, to a completely random looking function over the phase space. The Husimi of the complementary projector, $\hat{P}_2$ will have

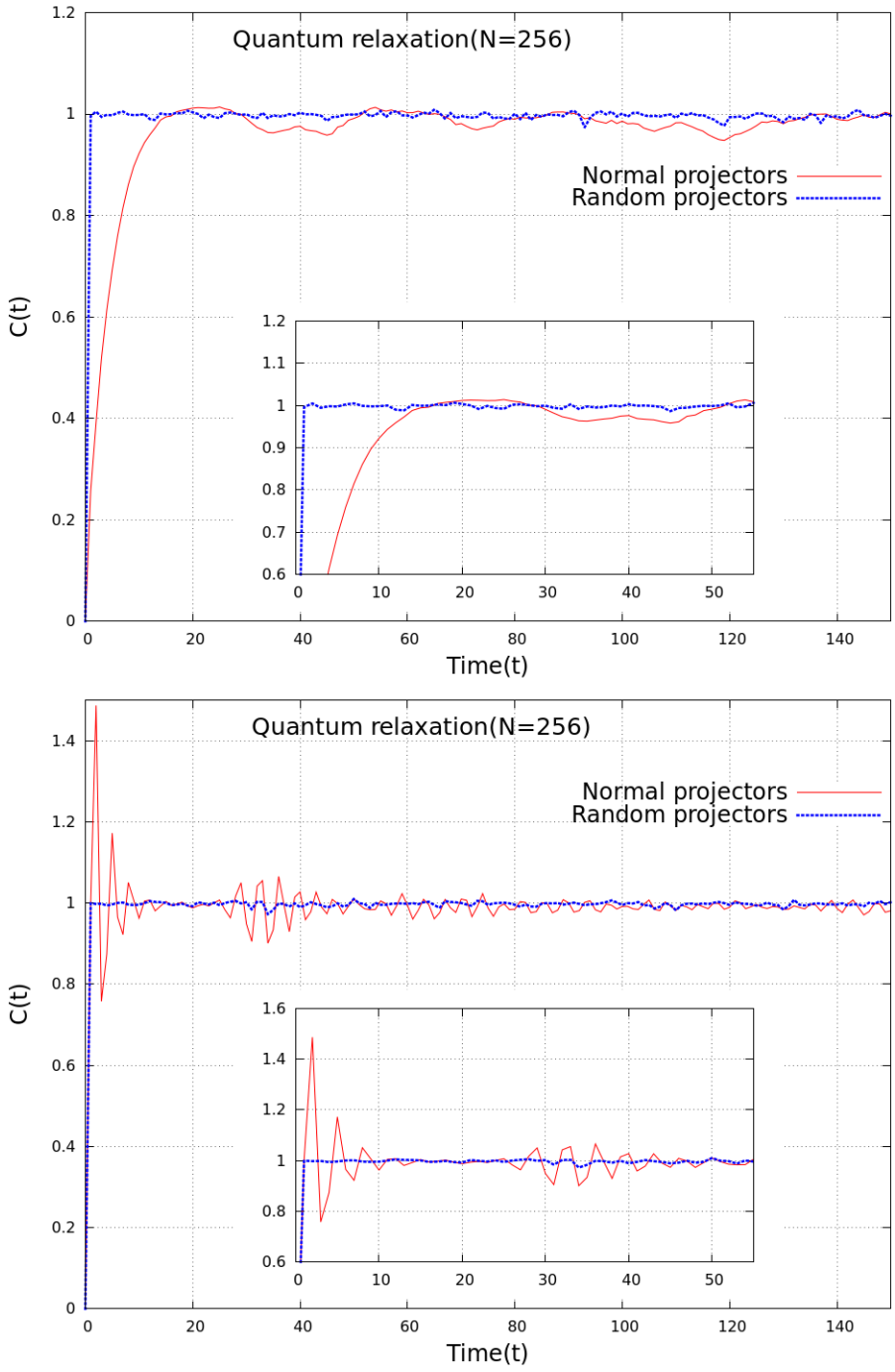

Figure 3.9: Relaxation of a pure CUE random transformation on the projectors, for the three-baker(above) and the lazy-baker(below). $N = 256$.

a complementary phase space structure under the same transformation. Therefore, intuitively we can remark that since, the classical analogue of the random projector is

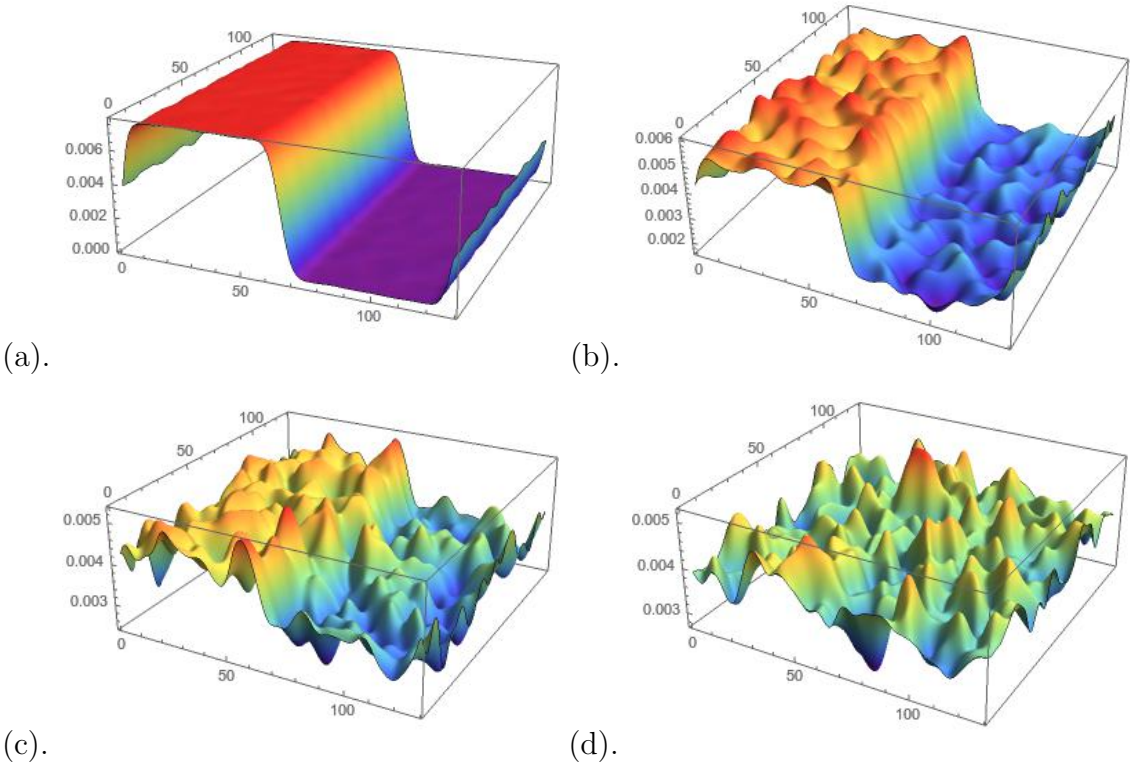

Figure 3.10: Husimi representation of a random unitary transformation on projector $\hat{P}_1$ for $\frac{\epsilon}{\sqrt{N}}$ = (a) 0.0, (b) 0.5, (c) 0.7 and (d) 1.0. $N = 128$

such a randomly distributed function, it is perfectly set-up to immediately approach relaxation even after a single iteration of the map. For intermediate values of $\frac{\epsilon}{\sqrt{N}}$ we can still see a resemblance of the structure of the normal projectors. This is probably the reason for the hint of R-P resonances in it's relaxation noted earlier.

For the case of the standard map, the position basis is not special and no specific characteristic of the relaxation profile is observed, indicative of the same. The *Ruelle-Pollicott* resonances for the standard map are not known yet and therefore a comparison is not possible. Moreover, R-P resonances for any general dynamical system is not a straight-forward calculation. The quantum relaxation of the standard map has been studied earlier by Lakshminarayan in [26], where the time-average of relaxation was studied. In this thesis we use the standard map to study the relaxation of random projectors averaged over the CUE.

3.3 Average of relaxation over CUE

In the previous chapter, we have analytically calculated the average of the relaxation over the *circular unitary ensemble*(CUE) when using random projectors. We had also presented an exact expression for the average of the relaxation fluctuation when the initial projectors are orthogonal to each other (eqn.2.43). The expression for

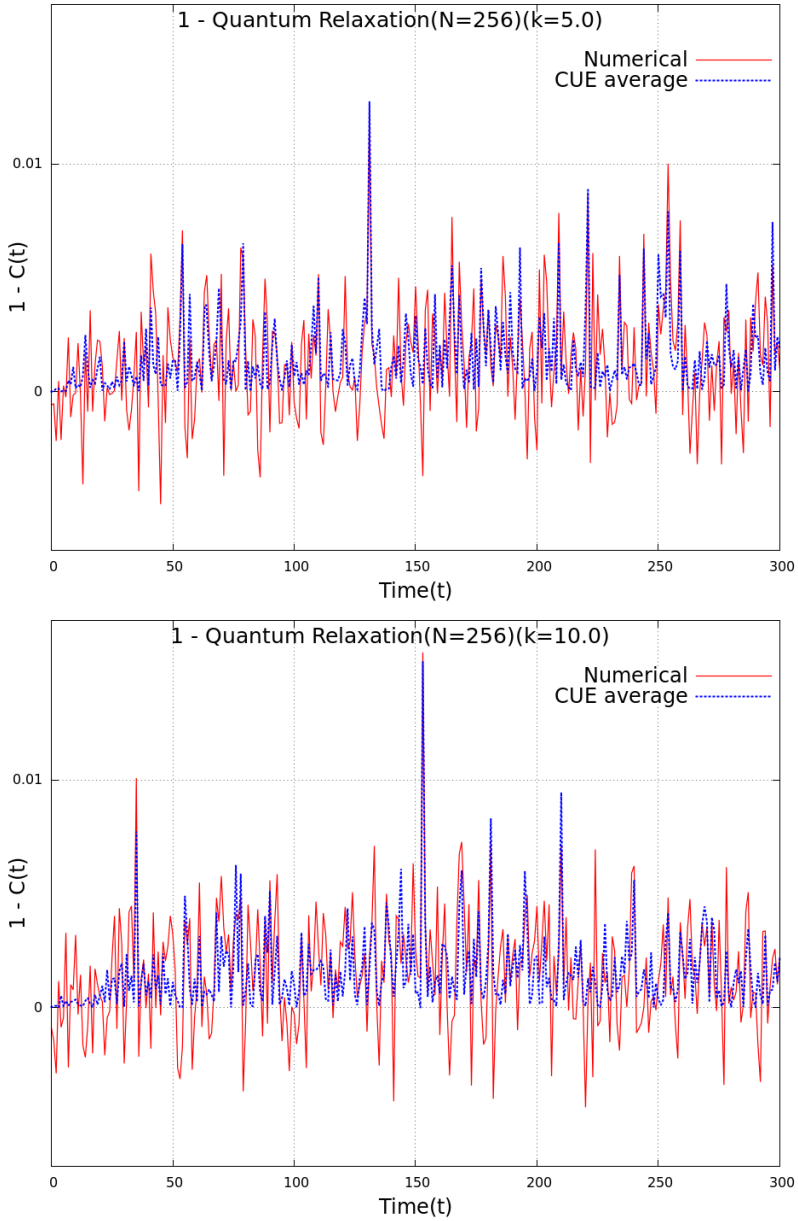

Figure 3.11: Plot of relaxation fluctuation of random projectors(blue) and the average of the relaxation fluctuation (epn.2.43) for the standard map. $N = 256$ and $k = 5, 10$

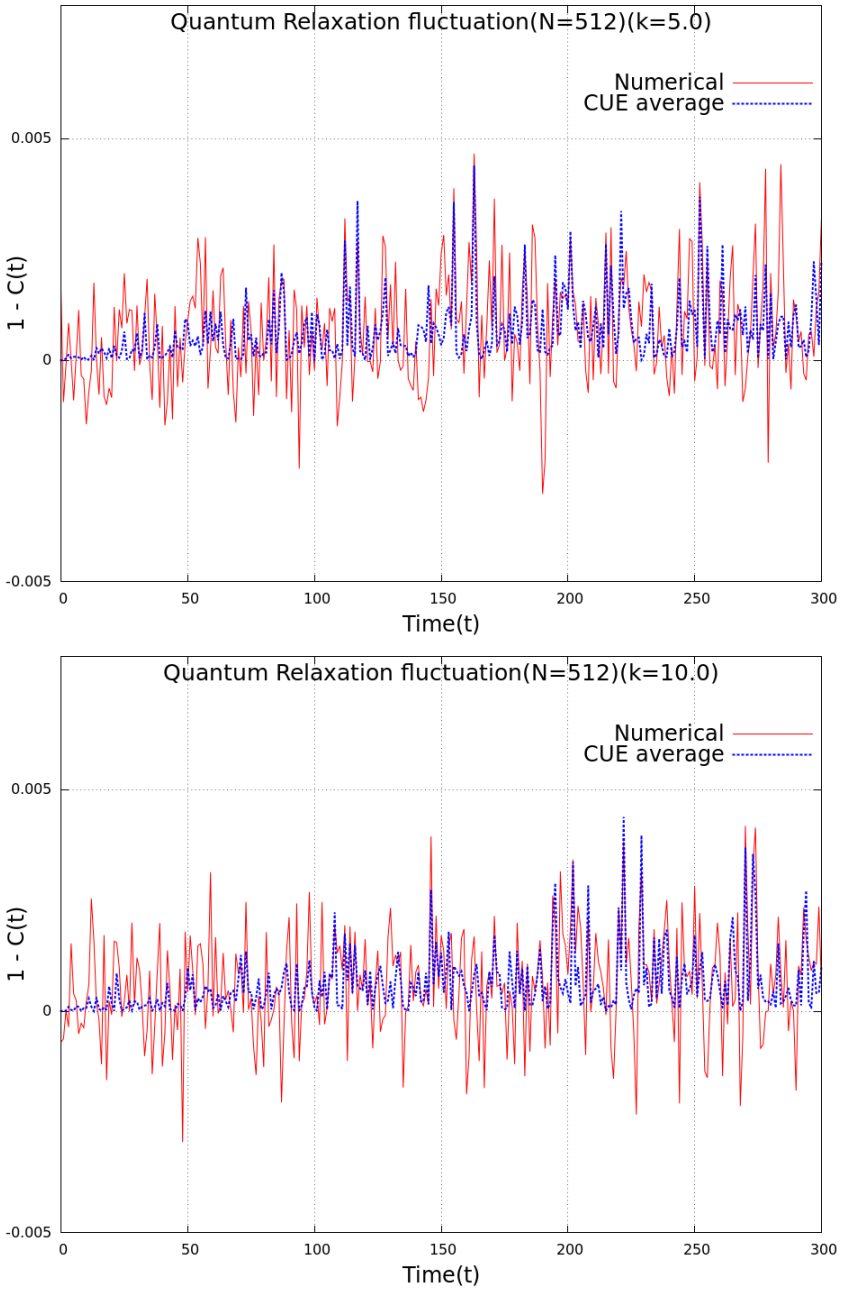

Figure 3.12: Plot of relaxation fluctuation of random projectors(blue) and the average of the relaxation fluctuation (eqn.2.43) for the standard map. $N = 256, 512$ and $k = 5, 10$

the relaxation fluctuation had an explicit dependence on the *spectral form-factor* (eqn.2.44) and we can calculate this numerically by simply performing a sum over the relevant powers of the eigenvalues. We will now plot the numerical values of

fluctuations of the relaxation of random projectors and it's analytical averaged value. In the above figures, we observe that the relaxation fluctuations of random projectors has clear structures reminiscent of the averaged value. Therefore, we can indeed say that there is some order to the behavior of the relaxation although not apparent.

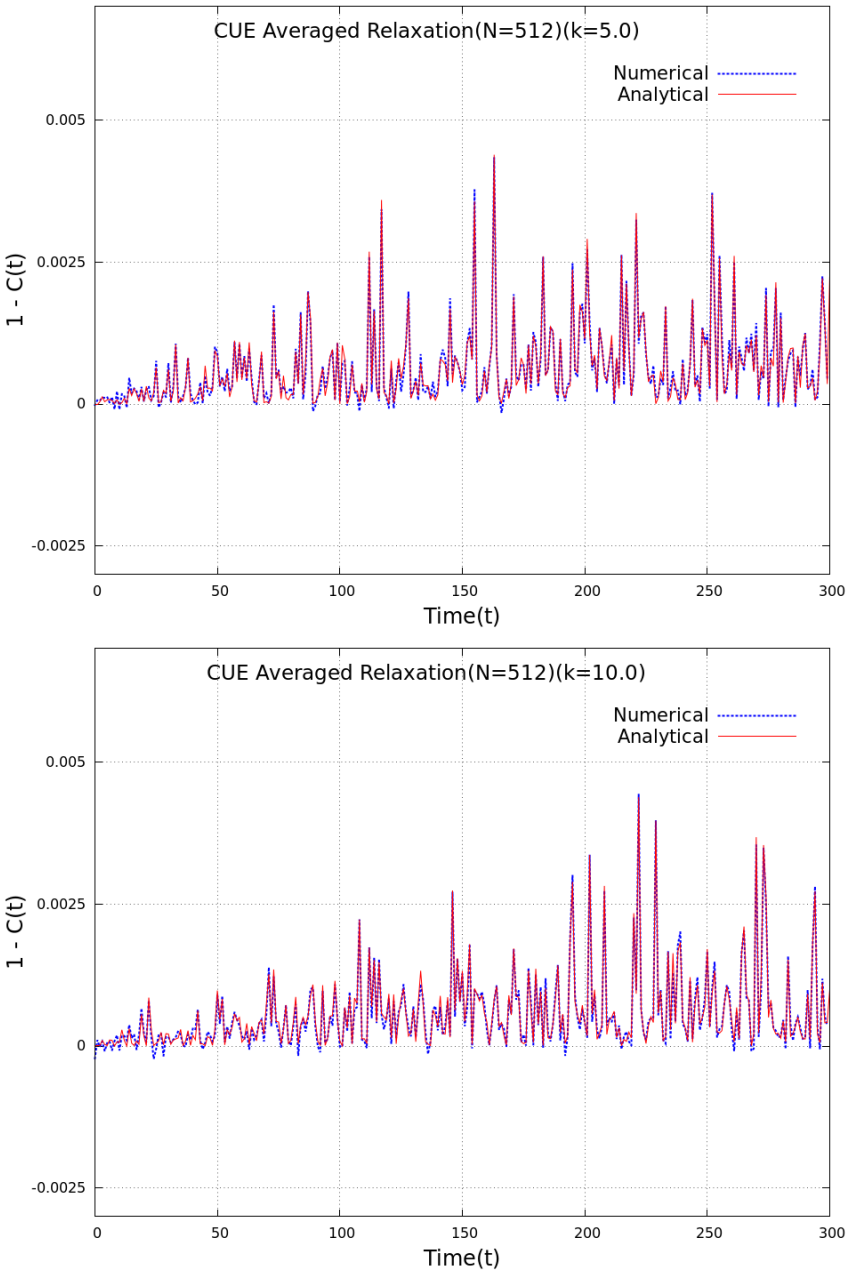

Figure 3.13: Plot of the relaxation fluctuation about equilibrium and it's CUE averaged value (eqn.2.43) for the standard map when $k = 5$(top) and 10(bottom) and $N = 512$

In the above figure, a numerical average of the relaxation fluctuations over 100 different realizations of unitary transformations on the projectors has been plotted. The numerical averages of the relaxation seem to exactly match with the expected value of the average. The values of $k = 5, 10$ correspond to the cases when there is a "mixed" phase space and complete chaos over the phase space respectively. Similar observations for other values of k have also been observed.

As noted in the previous chapter, the spectral form factor is not self-averaging [37] and hence we see fluctuations in the averaged quantity. However, we do know that the fluctuations of the spectral form-factor are due to contributions from short periodic-orbits [37] based on semiclassical studies. But one unsettling feature of the above figures is the fact that, the value of analytically averaged relaxation fluctuations is always positive, whereas the relaxation fluctuations in general can be both positive and negative. To make this a little more clear, we have performed an additional numerical average of both the quantities over a small range of k around a given value. This is like the average of the relaxation fluctuations performed over it's respective random matrix ensemble. The form-factor averaged over the COE has a definite analytical structure and the normalized expression was mentioned in the last chapter, eqn.2.45.

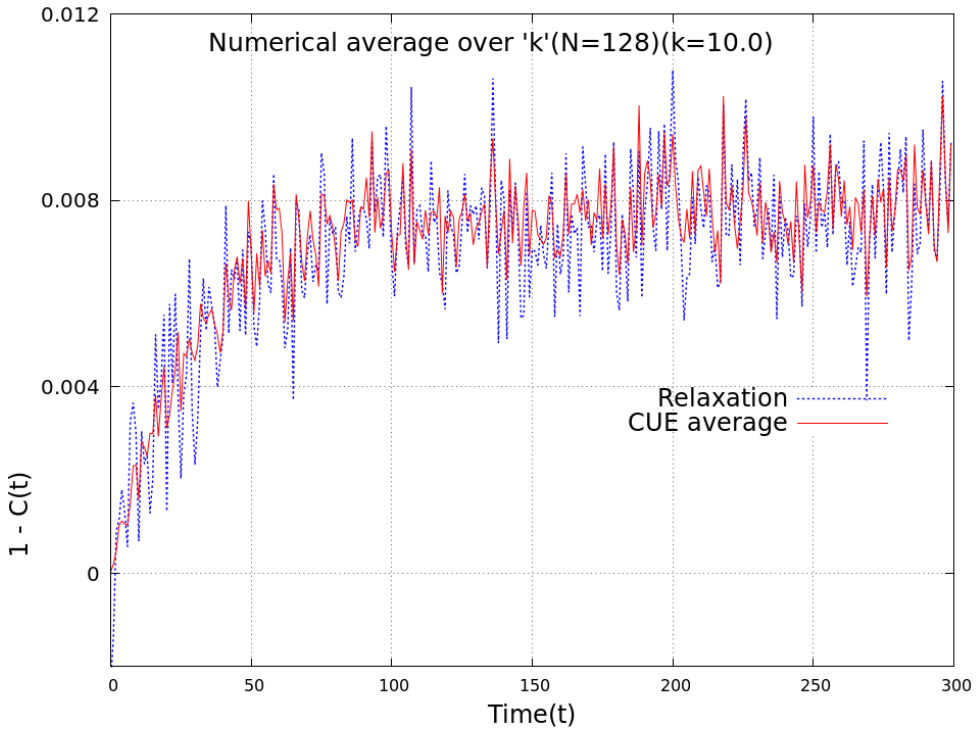

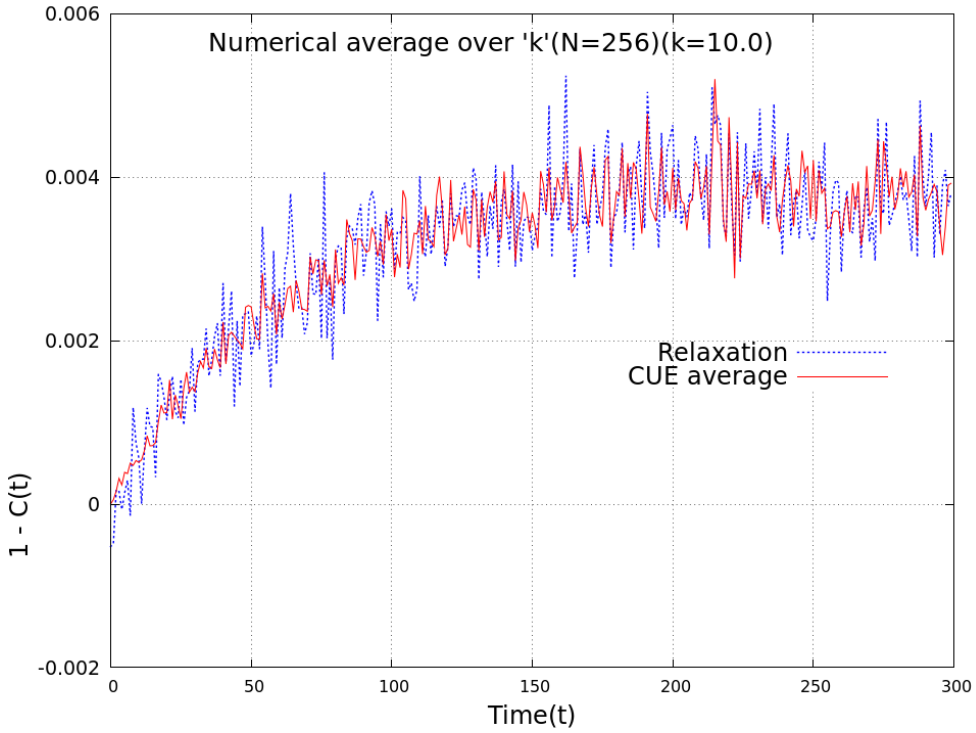

Figure 3.14: Numerical average over k, of the relaxation fluctuation and it's CUE average. The averages were calculated for 100 different values of k uniformly sampled over a unit range around $k = 10$ and $N = 128, 256$ respectively.

Since the relaxation fluctuations is just linearly dependent on the spectral form-factor, we can expect it to have a similar structure as the spectral-form factor averaged over the CUE. As expected, fig.3.14 shows the numerical average over k having a similar structure predicted for the spectral form-factor. The form-factor logarithmically approaches the value of unity, i.e $|\operatorname{Tr}(U^t)|^2 = N$ for $t > N$. From the expression for the relaxation fluctuations, $1 - \langle c(t)\rangle = 1/(N+1)$ for $t > N$. This implies that the relaxation fluctuation should approach $\frac{1}{(N+1)}$ for long time. When the value of $N = 128$ and 256, the value of $\frac{1}{(N+1)}$ should approximately be 0.00775 and 0.00389 respectively. This agrees with what we observe in the plot.

Chapter 4

Conclusion and outlook

In this thesis, we have analyzed the relaxation to equilibrium of bounded chaotic systems on the unit square. Relaxation to equilibrium has been quantified by a mixing in phase space. This mixing has been described as the overlap of two subsets belonging to the phase space as one of them is evolved in time. Using the property of mixing in dynamical systems, the expression to calculate the relaxation has been discussed and quantified as a growth of correlation over time, using characteristic phase space functions. Classically, this mixing in phase space is described by the *Ruelle-Pollicott* resonances. These *Ruelle-Pollicott* resonances have been calculated for the Lazy-baker map, by defining Markov partitions to represent the dynamics of the map symbolically. Having found the R-P resonances, we derive the classical relaxation law between subsets defined using the Markov partitions.

The analogous expression to quantify mixing between subspaces in Hilbert space has been discussed in detail. Projectors have been used as the analogues of the characteristic phase space functions and the corresponding correlations has been defined using them. Projectors onto subspaces and the trace of their overlap as one of them evolves in time is presented as the expression for the "quantum mixing" or the quantum correlation. The evolution in time is given by the Floquet operator which has been derived previously for all the system covered in this thesis. Using this expression, an equivalence of the quantum relaxation with classical relaxation law for short time has been shown numerically for different initial projectors in the case of the Lazy-baker.

Later, the case of relaxation of "random" projectors has been discussed. Random projectors are defined as random unitary transformation acting on otherwise simple

projectors. Random unitary matrices and numerical ways to generate them have been mentioned in brief including a particular construct to quantify it's randomness. The relaxation of such random projectors under time evolution of the quantum system has been observed to be immediate for the lazy-baker and three-baker. The immediate relaxation is in complete contrast to the quantum mixing without any such transformations on the projectors. The action of random unitary transformations on the projectors and consequently on the relaxation is thus shown to slowly erase any signature of the R-P resonances that were present otherwise. Using a particular construct of the random unitary transformations to discern it's degree of randomness, we see a slow departure from the classical relaxation. However, in the course of the transition to a completely random transformations, we do observe the relaxation to be influenced by the R-P resonances of the classical map, till any such signature is completely destroyed. Thus random unitary transformations on projectors are therefore shown to entail a maximal mixing of the phase space with the phase space representations of the random projectors indicating the same.

The relaxation of these random projectors has been averaged over the ensemble of all such random unitary transformations, namely the *circular unitary ensemble* (CUE). The average could be calculated analytically thanks to the specific structure of the quantum correlation. Such an average is shown to be independent of the partitions as long as they are orthogonal to each other. The expression for the quantum relaxation averaged over the ensemble of the random unitary matrices is shown to explicitly depend on a well studied quantity, namely the *spectral form-factor*. The form-factor is a property of random matrix ensembles and semiclassical studies have provided an analytical expression for the form-factor in terms of the periodic-orbit theory. The spectral form-factor approaches the value of 1 asymptotically and using this, the asymptotic limit of the averaged relaxation fluctuations has been shown to be $1/(N+1)$, when the projectors are orthogonal. This shows a reluctance of the quantum system to approach complete relaxation. In the semiclassical limit, this averaged relaxation fluctuations approaches 0 as it should, since it has to reflect the expected classical law. The results of numerical calculations also suggest an agreement with the analytical result.

Random unitary transformations have been studied since long time back and have been primarily restricted to random matrix theory and Quantum chaos. In recent times, it has been studied in the field of Quantum information in conjunction with

random-operators [43], superdense coding [44], quantum cryptography [45, 46], dynamics of quantum networks [47], black hole dynamics [48] and an associated scrambling of quantum information [49]. These studies have huge implications on the realization of a quantum computer and are therefore replete with opportunities.

Bibliography

[1] N Meenakshisundaram. *Studies in Quantum Chaos: From an almost exactly solvable model to Hypersensitive operators*. PhD thesis, INDIAN INSTITUTE OF TECHNOLOGY MADRAS, 2010.

[2] Robert C Hilborn and JC Sprott. Chaos and nonlinear dynamics: an introduction for scientists and engineers. *American Journal of Physics*, 62(9):861–862, 1994.

[3] Martin C Gutzwiller. *Chaos in classical and quantum mechanics*, volume 1. Springer Science & Business Media, 2013.

[4] Fritz Haake. *Quantum signatures of chaos*, volume 54. Springer Science & Business Media, 2013.

[5] Michael Berry. Quantum chaology, not quantum chaos. *Physica Scripta*, 40(3):335, 1989.

[6] Oriol Bohigas, Marie-Joya Giannoni, and Charles Schmit. Characterization of chaotic quantum spectra and universality of level fluctuation laws. *Physical Review Letters*, 52(1):1, 1984.

[7] Madan Lal Mehta. *Random matrices*, volume 142. Academic press, 2004.

[8] Arul Lakshminarayan. Entangling power of quantized chaotic systems. *Physical Review E*, 64(3):036207, 2001.

[9] Erich Joos, H Dieter Zeh, Claus Kiefer, Domenico JW Giulini, Joachim Kupsch, and Ion-Olimpiu Stamatescu. *Decoherence and the appearance of a classical world in quantum theory*. Springer Science & Business Media, 2013.

[10] Wojciech Hubert Zurek and Juan Pablo Paz. Decoherence, chaos, and the second law. *Physical Review Letters*, 72(16):2508, 1994.

[11] Nandor L Balazs and André Voros. The quantized baker's transformation. *Annals of Physics*, 190(1):1–31, 1989.

[12] Marcos Saraceno. Classical structures in the quantized baker transformation. *Annals of Physics*, 199(1):37–60, 1990.

[13] G Casati, BV Chirikov, FM Izrailev, and J Ford. Lecture notes in physics, vol. 93, 1979.

[14] Felix M Izrailev. Simple models of quantum chaos: spectrum and eigenfunctions. *Physics Reports*, 196(5-6):299–392, 1990.

[15] P Leboeuf, J Kurchan, M Feingold, and DP Arovas. Phase-space localization: topological aspects of quantum chaos. *Physical review letters*, 65(25):3076, 1990.

[16] Michael V Berry, Nandor L Balazs, Michael Tabor, and André Voros. Quantum maps. *Annals of Physics*, 122(1):26–63, 1979.

[17] A Lakshminarayan and NL Balazs. Relaxation and localization in interacting quantum maps. *Journal of Statistical Physics*, 77(1):311–344, 1994.

[18] A Lakshminarayan and NL Balazs. The classical and quantum mechanics of lazy baker maps. *Annals of Physics*, 226(2):350–373, 1993.

[19] Joseph Berkovitz, Roman Frigg, and Fred Kronz. The ergodic hierarchy, randomness and hamiltonian chaos. *Studies in History and Philosophy of Science Part B: Studies in History and Philosophy of Modern Physics*, 37(4):661–691, 2006.

[20] David Ruelle. Locating resonances for axioma dynamical systems. *Journal of statistical physics*, 44(3):281–292, 1986.

[21] Brian Swingle, Gregory Bentsen, Monika Schleier-Smith, and Patrick Hayden. Measuring the scrambling of quantum information. *Physical Review A*, 94(4):040302, 2016.

[22] Robert L Devaney et al. *An introduction to chaotic dynamical systems*, volume 13046. Addison-Wesley Reading, 1989.

[23] Lawrence Markus and Kenneth Ray Meyer. *Generic Hamiltonian dynamical systems are neither integrable nor ergodic*, volume 144. American Mathematical Soc., 1974.

[24] Vladimir Igorevich Arnol'd and André Avez. Ergodic problems of classical mechanics. 1968.

[25] John M Greene. A method for determining a stochastic transition. *Journal of Mathematical Physics*, 20(6):1183–1201, 1979.

[26] Arul Lakshminarayan. Relaxation fluctuations about an equilibrium in quantum chaos. *Physical Review E*, 56(3):2540, 1997.

[27] David Ruelle. Resonances of chaotic dynamical systems. *Physical review letters*, 56(5):405, 1986.

[28] Yves Elskens and Raymond Kapral. Reversible dynamics and the macroscopic rate law for a solvable kolmogorov system: The three bakers' reaction. *Journal of statistical physics*, 38(5-6):1027–1049, 1985.

[29] Shashi CL Srivastava and Arul Lakshminarayan. Records in the classical and quantum standard map. *Chaos, Solitons & Fractals*, 74:67–78, 2015.

[30] Kin'ya Takahashi. Wigner and husimi functions in quantum mechanics. *Journal of the Physical Society of Japan*, 55(3):762–779, 1986.

[31] Stephan Tornier. Haar measures. *https://people.math.ethz.ch/ torniers*, 2014.

[32] Karol Zyczkowski and Marek Kus. Random unitary matrices. *Journal of Physics A: Mathematical and General*, 27(12):4235, 1994.

[33] Francesco Mezzadri. How to generate random matrices from the classical compact groups. *arXiv preprint math-ph/0609050*, 2006.

[34] Joshua Wilkie and Paul Brumer. Time-dependent manifestations of quantum chaos. *Physical review letters*, 67(10):1185, 1991.

[35] Zbigniew Puchała and Jarosław Adam Miszczak. Symbolic integration with respect to the haar measure on the unitary group in mathematica. *arXiv preprint arXiv:1109.4244*, 2011.

[36] E Brézin and S Hikami. Spectral form factor in a random matrix theory. *Physical Review E*, 55(4):4067, 1997.

[37] RE Prange. The spectral form factor is not self-averaging. *Physical review letters*, 78(12):2280, 1997.

[38] G. Berkolaiko. LETTER TO THE EDITOR: Diagonal approximation of the form factor of the unitary group. *Journal of Physics A Mathematical General*, 39:L77–L84, January 2006.

[39] Hans-Jürgen Stöckmann. Quantum chaos: an introduction, 2000.

[40] Conrad Sanderson and Ryan Curtin. Armadillo: a template-based c++ library for linear algebra. *Journal of Open Source Software*, 1(2):26–32, 2016.

[41] T Williams, C Kelley, HB Bröker, J Campbell, R Cunningham, D Denholm, E Elber, R Fearick, C Grammes, and L Hart. Gnuplot 4.6: An interactive plotting program, 2012. *URL http://www. gnuplot. info*.

[42] N Meenakshisundaram and Arul Lakshminarayan. Multifractal eigenstates of quantum chaos and the thue-morse sequence. *Physical Review E*, 71(6):065303, 2005.

[43] Joseph Emerson, Yaakov S Weinstein, Marcos Saraceno, Seth Lloyd, and David G Cory. Pseudo-random unitary operators for quantum information processing. *Science*, 302(5653):2098–2100, 2003.

[44] Aram Harrow, Patrick Hayden, and Debbie Leung. Superdense coding of quantum states. *Physical review letters*, 92(18):187901, 2004.

[45] Patrick Hayden, Debbie Leung, Peter W Shor, and Andreas Winter. Randomizing quantum states: Constructions and applications. *Communications in Mathematical Physics*, 250(2):371–391, 2004.

[46] Charles H Bennett, Patrick Hayden, Debbie W Leung, Peter W Shor, and Andreas Winter. Remote preparation of quantum states. *IEEE Transactions on Information Theory*, 51(1):56–74, 2005.

[47] Jaroslav Novotnỳ, Gerd Alber, and Igor Jex. Random unitary dynamics of quantum networks. *Journal of Physics A: Mathematical and Theoretical*, 42(28):282003, 2009.

[48] Patrick Hayden and John Preskill. Black holes as mirrors: quantum information in random subsystems. *Journal of High Energy Physics*, 2007(09):120, 2007.

[49] Winton Brown and Omar Fawzi. Scrambling speed of random quantum circuits. *arXiv preprint arXiv:1210.6644*, 2012.